

High-resolution mass spec for metabolomic analysis

From lipidomics to cell bioenergetics, explore an integrated, multi-omics approach to metabolism



BROUGHT TO YOU BY INDEPENDENT SCIENCE PUBLISHER

SelectScience®

IN PARTNERSHIP WITH





Introduction

Since its first use to demonstrate the existence of isotopes, the application of mass spectrometry (MS) has expanded immeasurably, and its practitioners are to be found in almost every analytical laboratory. Driven by ever-increasing demand for greater performance and speed, particularly for analyzing complex biological samples, MS technology has continued to improve and, through coupling with other technologies (chromatography and data processing software), to yield the cutting-edge, high-throughput workflows we see today.

In this eBook, we look at some of the wide-ranging applications of the latest MS technology and workflows used to solve some of the most challenging analytical challenges faced by biologists working in metabolic profiling. In particular, we focus on Agilent Technologies' latest mass spectrometer, the [6546 LC/Q-TOF](#), an instrument designed to provide wide dynamic range while simultaneously providing high resolution independent of acquisition speed. Discover

Contents

- Gaining higher confidence and throughput in metabolite analysis
- A multi-omics approach to metabolism
- Extracellular flux analysis in LPS-stimulated macrophages
- Improving coverage of the plasma lipidome with Lipid Annotator software
- Lipid profiling workflow demonstrates disrupted lipogenesis in leukemia cells
- From metabolomics to mechanisms with mass spectrometry
- Featured products

how its integration in workflows can yield information on metabolic networks, cell bioenergetics, lipid function and much more.

Metabolomics

High-resolution MS is being applied to the challenges presented by high-throughput metabolomics to unravel the intricacies of metabolic networks:

- Apply Agilent's 6546 LC/Q-TOF to analyze a [complex biological matrix](#) with no prior separation for improved sample throughput. In analyzing the complex metabolome of the bacterium *E. coli*, Agilent's technology permits more metabolic features to be found, profiled and annotated.
- Learn how the shift from needing to measure not only metabolite levels but [reaction rates or metabolic flux](#) has driven MS technology forward and now allows biologists to gain insight into what is happening inside cells under various challenges, be they mutations, drug treatments or chemical agents. Refinement of Agilent's [6546 LC/Q-TOF](#) technology has made the system especially well-suited for simultaneously measuring low abundance peaks in the presence of high-intensity signals.
- View a [webinar](#) detailing how to profile large cohorts with tens of thousands of samples and how to shift from data generation to the functional interpretation of results, and exploring novel trends in metabolomic and ¹³C metabolic flux analysis.

Immunometabolism

Gaining access in real time to the bioenergetic state of a cell is a genuine challenge that can provide valuable insight into cell health and function. Discover a workflow

in which Agilent's [6546 LC/Q-TOF](#) with [MassHunter](#) VistaFlux software (used to perform ¹³C stable isotope tracing analysis), is combined with Seahorse XF technology to elucidate the response of [macrophages to lipopolysaccharide treatment](#). This workflow can uncover the molecular mechanisms of cell metabolism in response to external triggers or genetic manipulation.

Lipidomics

High-resolution MS finds multiple applications in lipid profiling, in particular where the comprehensive characterization of a large and diverse set of lipid species is required that spans a wide concentration with a biological sample. It allows researchers to overcome the shortcomings of earlier lipidomics techniques which suffered from limitations in resolution and reduced dynamic range. Discover:

- Improved [characterization of the plasma lipidome](#) by using iterative MS/MS data acquisition combined with Agilent's [MassHunter](#) Lipid Annotator software utilizing the [6546 LC/Q-TOF](#). Iterative MS/MS data can be used by Agilent Lipid Annotator software as part of a comprehensive lipidomics workflow.
- [Characterize lipid alterations](#) in acute myeloid leukemia cells subjected to different drug treatments, through the application of a comprehensive lipidomics profiling workflow. Key to the workflow is the integration of Agilent's [MassHunter](#) Lipid Annotator software with the [6546 LC/Q-TOF](#). This workflow was able to reveal significant differences in lipid class abundance not previously reported and was more comprehensive than a traditional shotgun-based lipidomics approach.

Agilent 6546 LC/Q-TOF: Gaining Higher Confidence and Throughput in Metabolite Analysis

Authors

Karen E. Yannell, PhD
Agilent Technologies, Inc.
Santa Clara, CA, USA

Christian Klein, PhD
Agilent Technologies, Inc.
Santa Clara, CA, USA

Nicola Zamboni, PhD
ETH Zurich
Zurich, Switzerland

Introduction

Metabolomics is constantly pushing the boundaries of complex analysis by mass spectrometry (MS). For high-throughput profiling of large sample collections, the trend is to accelerate chromatographic separation, and compensate the loss of temporal resolution with increased mass resolution and accuracy. In the most extreme form, chromatography is completely omitted to achieve thousands of injections per day with flow injection. Albeit powerful, high-throughput analysis of complex biological extracts is analytically challenging because of the wide dynamic range in concentration of metabolites in biological extracts. Whether or not chromatography is used, mass spectrometers must provide high resolution and mass accuracy over the full mass range, across many orders of dynamic range within the same scan, and at high acquisition rates.

This Technical Overview describes the capabilities of the Agilent 6546 LC/Q-TOF. The improved features of this instrument permit the analysis of a complex biological matrix with no prior separation. *E. coli* metabolome samples were prepared by ethanol extraction of bacteria growing exponentially on glucose minimal medium. These samples were analyzed by flow injection (1.5 μ L) using an Infinity II pump equipped with restrictive capillary. The 6546 LC/Q-TOF was tuned in negative mode, and data were acquired at 1.5 Hz over a m/z 50 to 1,000 mass range. The results show resolution $>30,000$ for analytes greater than m/z 118, improved mass accuracy, large spectral dynamic range, high sensitivity, and isotopic fidelity. Ultimately, this increased instrument performance allows more features to be found, profiled, and annotated in the *E. coli* sample.

Resolution and mass accuracy

The 6546 LC/Q-TOF achieves a resolution of at least 30,000 for ions above m/z 118, and greater than 60,000 for larger ions (m/z 1,521, $R = 60,000$). These values were reached in complex *E. coli* extracts regardless of the peak intensity and acquisition rate (Figure 1). Mass accuracy was largely within 0.3 mDa throughout the mass range, independent of peak intensity (Figure 2). This performance allows identification of molecular formulas without prior chromatographic separation and, therefore, increased throughput.

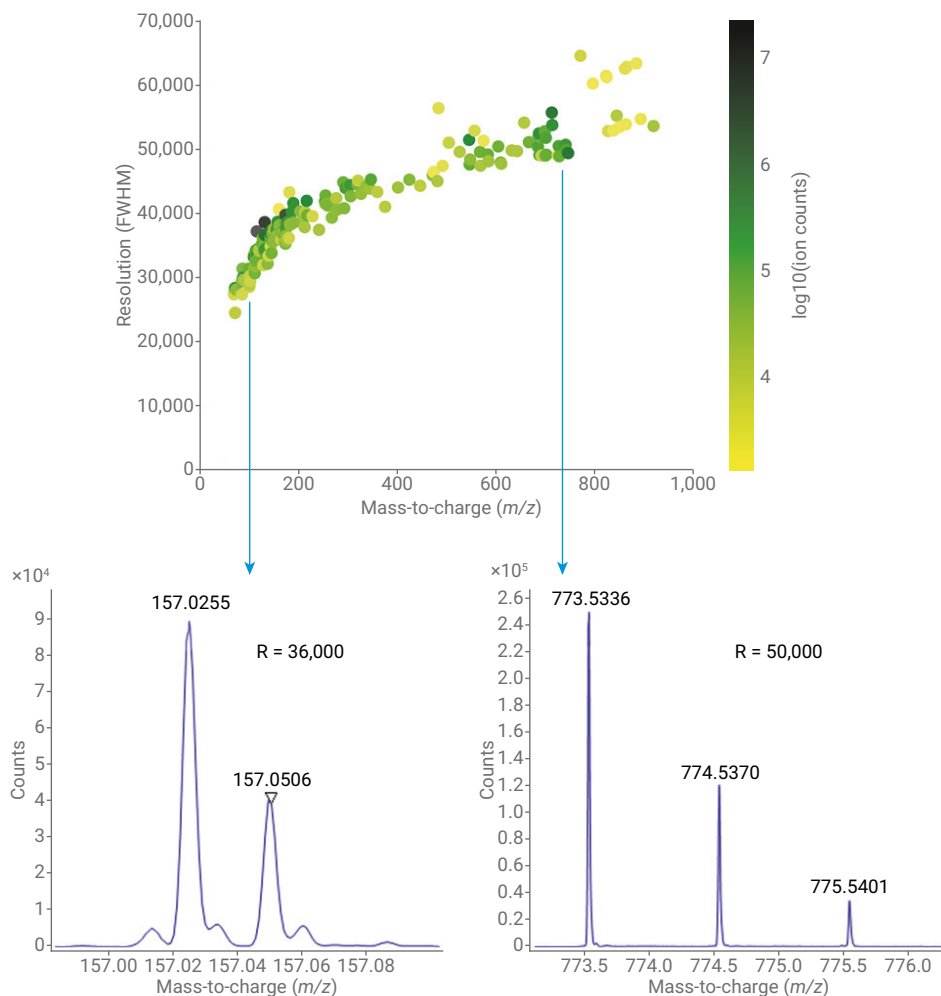


Figure 1. Resolution is plotted over the mass range for analytes in an *E. coli* sample analyzed by flow injection coupled with the 6546 LC/Q-TOF. Ion intensity is noted by color. Insets show the peak shapes for low and high mass ions.

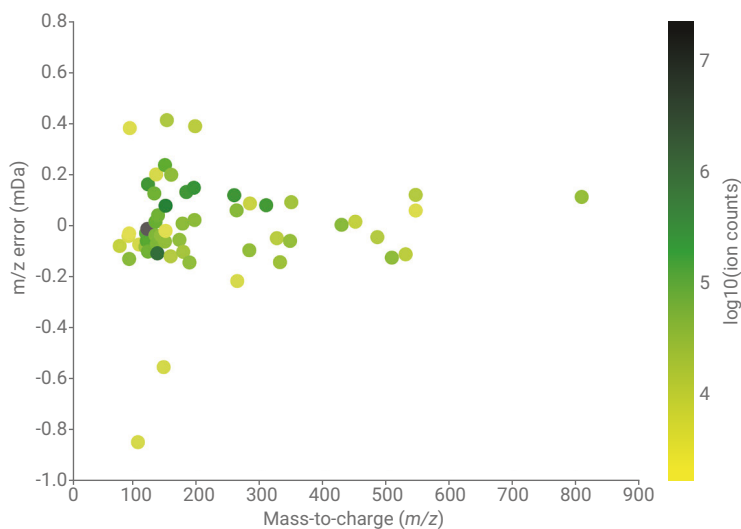


Figure 2. Mass error (mDa) is plotted over the mass range for extracted analytes in an *E. coli* sample analyzed by flow injection with the 6546 LC/Q-TOF. Ion intensity is noted by color.

Sensitivity and intrascan dynamic range

A dilution series of the *E. coli* extract was prepared in water, ranging from a 9X concentration to an 81-fold dilution. A concentration of 1X corresponds to the concentration routinely used on previous generations of Q-TOF instruments. Each sample was combined with the same amount (1X) of uniformly ^{13}C -labeled *E. coli* extract to mitigate diverging matrix effects in the recorded intensities. Triplicate injections were performed.

Analytes across the mass range were extracted, and their intensities were plotted to show the sensitivity of the 6546 LC/Q-TOF at low concentrations (or dilutions, Figure 3). The signal intensity was very stable at low concentrations, and error only began to increase around the 81-fold dilution. In the analysis of *E. coli* extracts at the standard 1X concentration, the sensitivity of the 6546 LC/Q-TOF enabled the detection of several metabolites similar to those obtained with the Agilent 6550 iFunnel Q-TOF LC/MS (Figure 4).

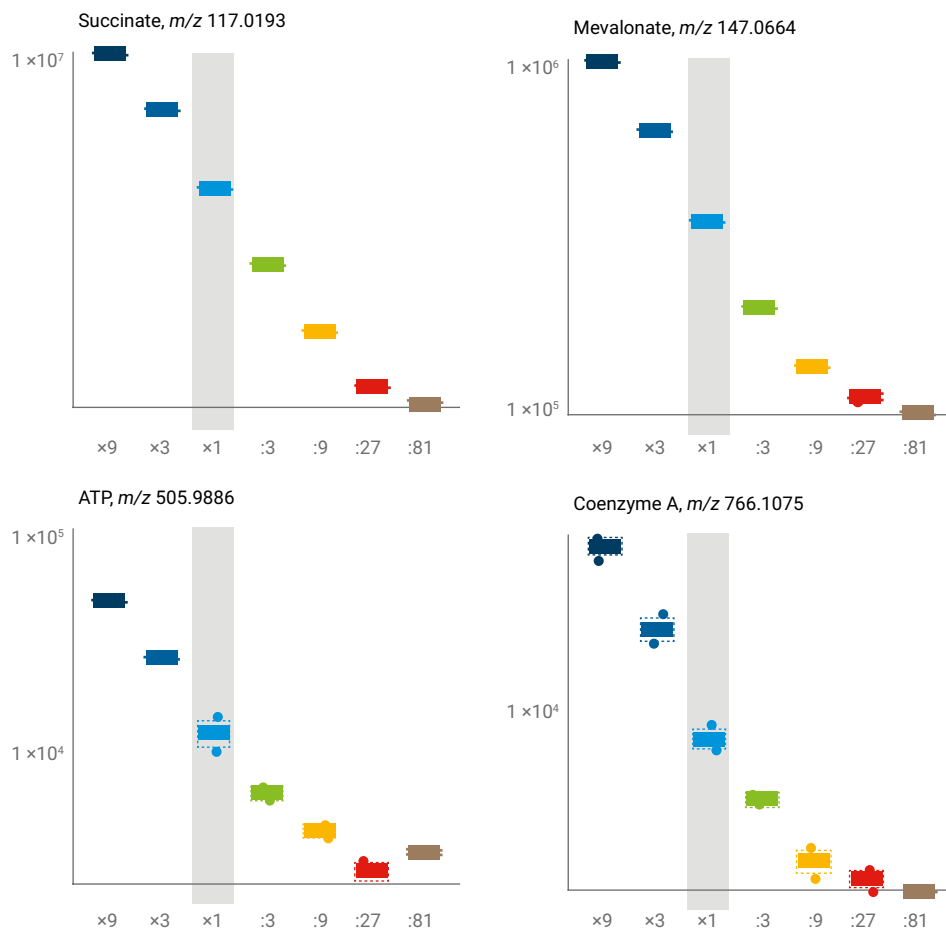
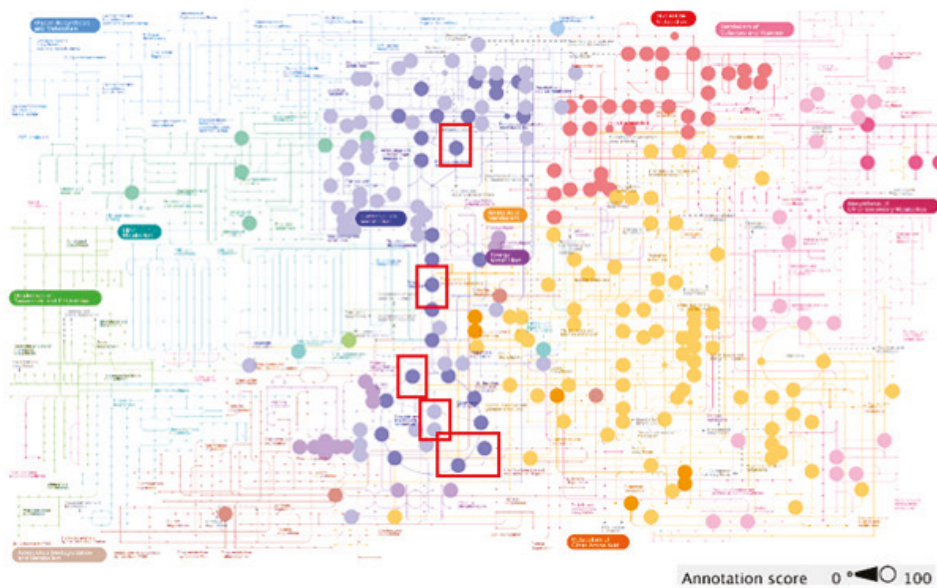


Figure 3. Ion intensity of four extracted analytes was plotted against the *E. coli* sample dilution. Error bars represent standard deviation when $n = 3$. The grey highlighted sample, 1X, is the standard concentration of *E. coli* samples used with earlier Q-TOF generations.

6546



6550

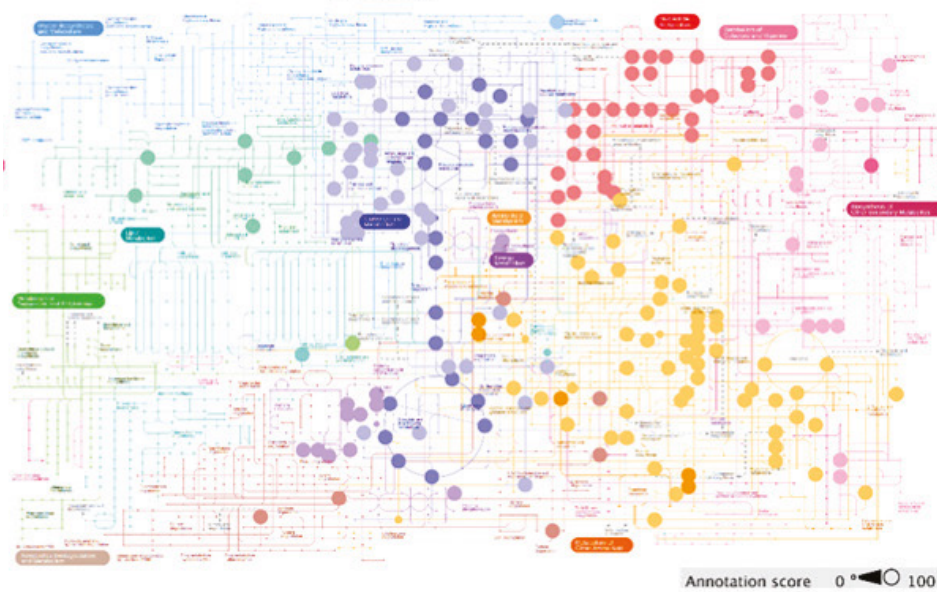


Figure 4. Metabolite map for features in the 1X *E. coli* sample when it was analyzed by the 6546 LC/Q-TOF and the 6550 iFunnel Q-TOF LC/MS. The colored circles represent features (or metabolites) detected in the sample. The 6546 LC/Q-TOF was able to identify more features (red squares) in several different metabolite classes compared to the 6550 Q-TOF LC/MS.

Additionally, the 6546 LC/Q-TOF has five orders of in spectrum dynamic range. This is more than could be explored using pure *E. coli* extracts, so the sample was spiked with $^{13}\text{C}_2$ -succinate. The novel 10 GHz analog to digital (ADC) acquisition system of the 6546 LC/Q-TOF enables precise detection of peaks in a complex sample spanning nearly four orders of magnitude within the same scan (Figure 5). This allows for quantification and identification of metabolites over the full dynamic range of complex extracts. This aspect is especially important when measuring complex matrices at high throughputs with little to no sample preparation or chromatography, since these samples often have both low and high intensity analytes of interest. In summary, the 6546 LC/Q-TOF provides continuous access to a full intrascan dynamic range without compromises in resolution, accuracy, sensitivity, or scan speed.

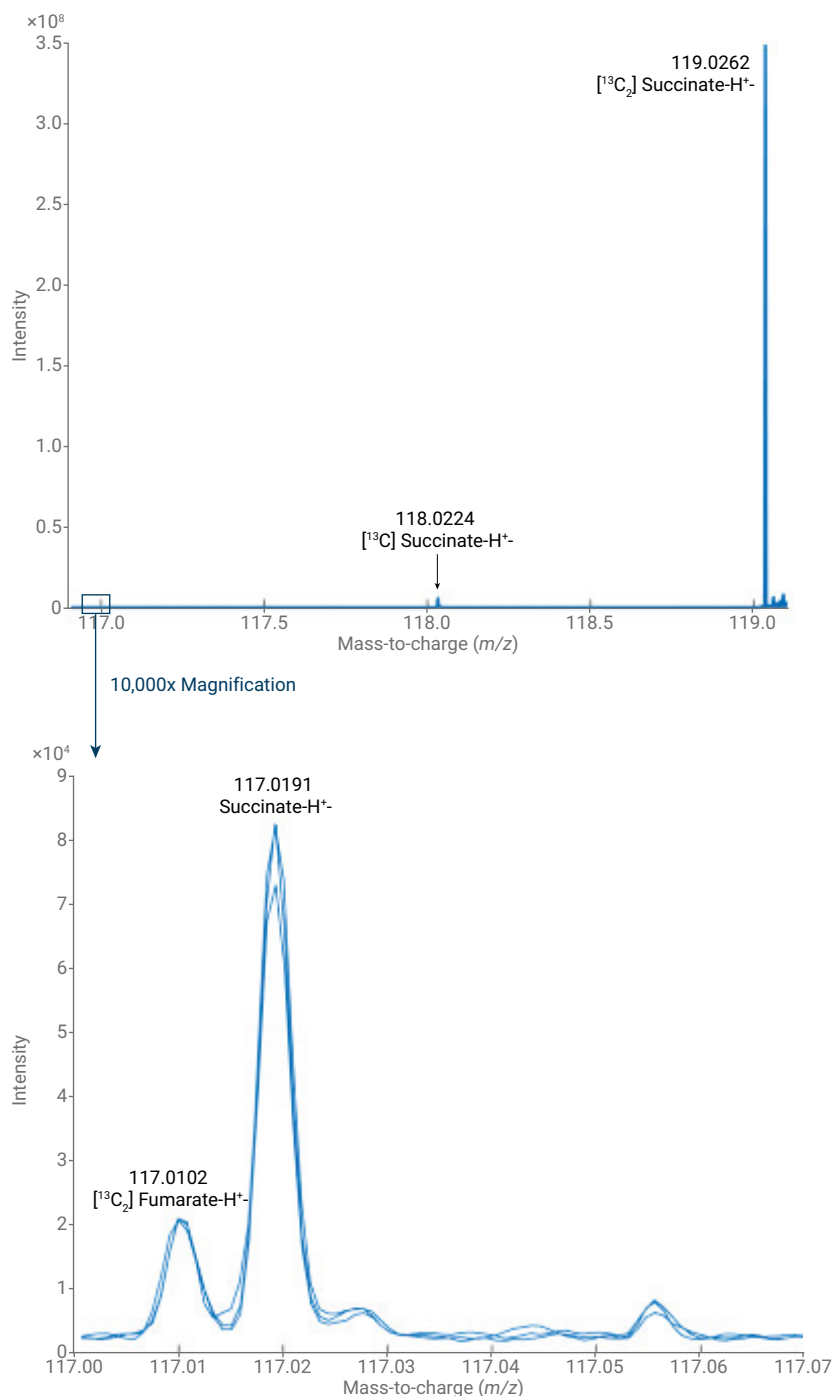


Figure 5. Intrascan dynamic range of the 6546 LC/Q-TOF. A $1\times$ ^{13}C -enriched *E. coli* extract was spiked with $^{13}\text{C}_2$ -succinate. Three technical replicates are superimposed. Despite the vast difference in intensities (10^4 to 10^8 counts), accuracy, and resolution are preserved and allow precise determination of both abundant and rare peaks within the same spectrum.

Isotopic resolution and fidelity

Further testing evaluated isotopic labeling performance of the 6546 Q-TOF LC/MS. In principle, accurate isotopic analysis depends on spectral resolution and linear dynamic range. Even in the absence of chromatographic separation, we found that the high resolution of the 6546 LC/Q-TOF enabled clear separation of most ^{13}C and ^2H isotopologues in crowded regions. Figure 6 illustrates this for the mass range with lowest resolution (m/z 100). The mass accuracy of <0.3 mDa ppm error across the whole range of masses and abundances enables prediction of molecular formulae with great confidence. For dozens of representative metabolites, the relative isotopic accuracy error (RIAE) was calculated. For most features, the RIAE was below 20 % (that is, in the range obtained with triple quadrupole detectors). Larger error was only observed for analytes with monoisotopic peaks nearing 10^4 intensity. These analytes have isotopes at or below 10^3 , and therefore in the baseline. The 6546 LC/Q-TOF robustly combines high resolution and isotopic fidelity by maintaining high accuracy in quantification.

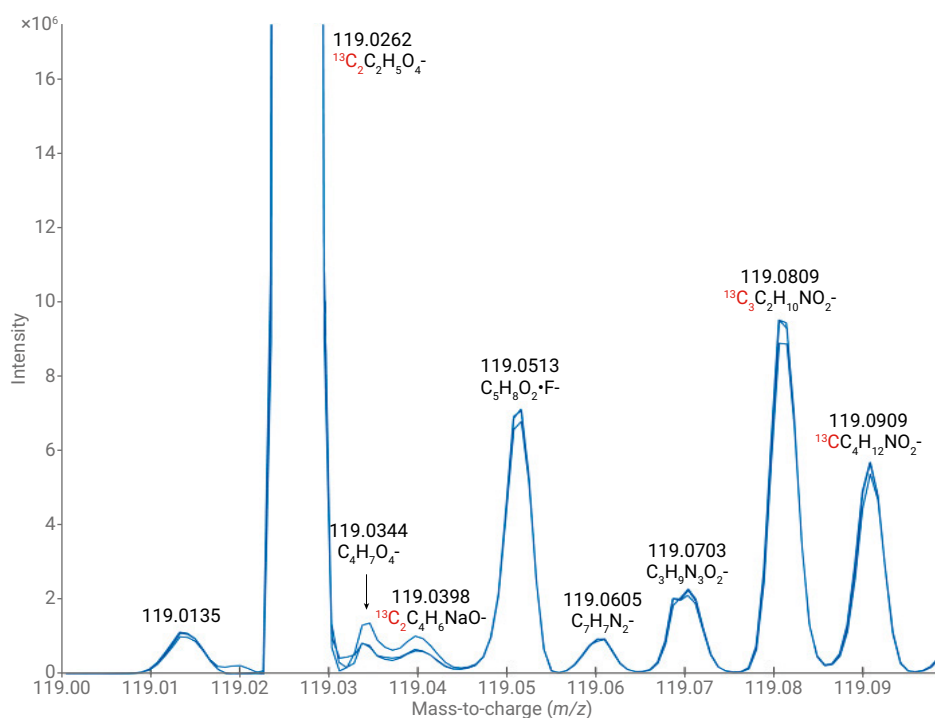


Figure 6. Spectral resolution of proximal ^{13}C and ^2H peaks in the low m/z range of an enriched *E. coli* extract measured by the 6546 LC/Q-TOF using flow injection.

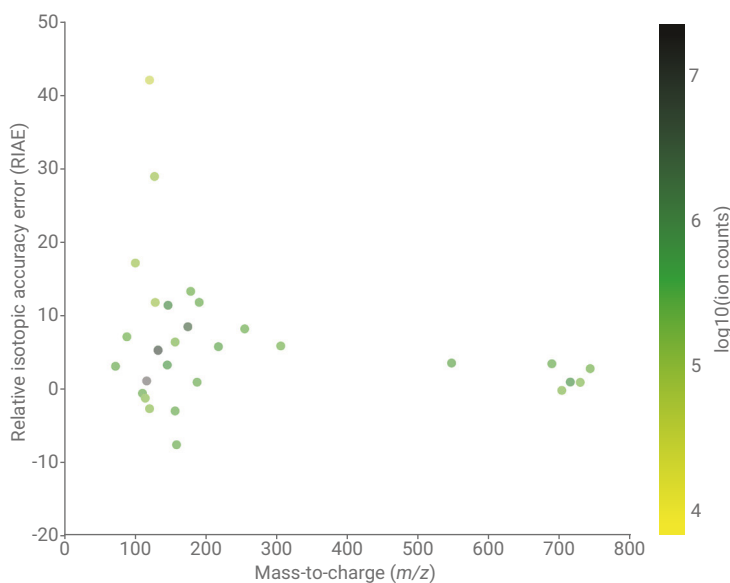


Figure 7. Accuracy of isotopic measurements. The RIAE reports the percent error for the ratio between theoretical and measured $M+1/M+0$. RIAE values <20 are considered excellent. Log of the sum of ion intensity over 10 scans is noted by color. Worse RIAE values are observed only for peak ions of low intensity, with $M+1$ ion counts of about 5 to 10 % of the monoisotopic peaks and falling in the range of the baseline.

www.agilent.com/chem

This information is subject to change without notice.

© Agilent Technologies, Inc. 2019
Printed in the USA, February 21, 2019
5994-0724EN

 **Agilent**
Trusted Answers

Agilent case study: Asking Nuanced Questions

Agilent Collaborator Takes an Integrated, Multi-omics Approach to Metabolism

Adam Rosebrock was feeling unsettled. For years he had been using genomics to study what cells do when they do, well ... what cells do. That is, which genes turn on or off as they go through cell division, for example, or various external insults.

Simply put, he was not getting enough information. So Rosebrock, a classically trained microbiologist and biochemist, began to expand the scope of his investigations.

“My push into metabolomics and mass spectrometry was my unsettled feeling coming to a head,” he says now. “I figured, if we wanted to measure what the cell was doing biochemically, we should just buckle down and measure metabolites directly.”

He started to focus on measuring small molecules and the direct output of metabolism using what he calls “kick-butt mass spectrometers and fantastic liquid chromatographs” from Agilent.

One of the biggest shifts over the past few years, Rosebrock notes, is that scientists began to measure not just metabolite levels but reaction rates, or metabolic flux.

“What that has required is really a shift in instrumentation, from thinking of mass spectrometry for metabolites as being a triple quadrupole question to being an accurate mass question,” he says. “My lab has been a proponent for accurate mass for a long time, and one of the reasons I’m really excited about Agilent’s portfolio right now is the continued excellence and refinement of the mass spectrometry platform, especially the Agilent 6546 Q-TOF system.”



Adam Rosebrock, PhD

Assistant Professor of Pathology
Director of Metabolomics Shared
Resource, Stony Brook Cancer Center
Renaissance School of Medicine
Stony Brook, New York
Co-founder, Maple Flavored Solutions

The platform is allowing Rosebrock to ask better, more nuanced questions.

“One of the most amazing ways that mass spectrometry has helped me as a biologist is getting insight into what’s happening inside cells as they are healthy and as they are unhealthy, either by mutation or by environmental exposure, or by treatment with drugs or chemical agents,” he says.

“For a long time, our phenotype, for geneticists in particular, was: Did my cell live or die? Or did my cell shrivel up and look really unhappy under the microscope? Those are broad descriptive terms. If the cell is dead, it can’t really tell you anything else,” Rosebrock notes. “Using mass spectrometry, though, we can start to ask about the biochemical state of the cell before the cell has really shut down and died. We can look at transitions between healthy cells and diseased cells. We can look at the changes inside the cell itself.”

Rosebrock says that he was blown away by the ability of the 6546 to measure compounds across a wide dynamic range when the system was first introduced. Through continued refinement, he adds, the system is now especially adept at simultaneously measuring low abundance peaks and dealing with high-intensity signals.

“Using the 6546, we can measure, at a given retention time, not just one mass-to-charge ratio, but we get a really fantastic high-resolution view, a high-dynamic range view, of different co-eluting analytes,” he says.

“We now have an easier time distinguishing crowded mass spectra and isolating individual isotopologues of our compounds in flux experiments using the 6546. Chromatography is still critical, but we have increased our biological feature counts and have better, more consistent, mass spectral peak shapes on the 6546. The system’s increased resolution gives us confidence in individual mass spectral features as being isotopologues rather than some coeluting interference. This has enabled us to generate higher-quality flux data, higher quality isotope-labeling data, and be more confident in the results we generate.”

Rosebrock’s lab analyzes the data using homegrown software along with what he describes as the unsung hero of Agilent’s metabolomics portfolio: MassHunter Profinder software.

“Cells maintain constant, homeostatic, levels of many metabolites across different environmental conditions and when faced with various intrinsic and extrinsic perturbations,” he says. “The underlying biochemistry is anything but static, however. We are finding that cells drastically change the rates of metabolic reactions in order to keep metabolite concentrations stable.”

To make matters even more complicated, scientists are also re-learning that metabolism is incredibly diversified and specialized.

“Even in our own bodies, there’s very different metabolism that occurs across different tissues. Your muscles are metabolically different from your liver or your kidneys. Even you and I will have differences in our metabolic processes—and there is genetic variation that underlies why your liver might work differently than my liver does,” Rosebrock says.

So he and his fellow research scientists are using everything they know and everything they can learn from microbiology, biochemistry, genetics, genomics, and metabolomics to understand the differences between individuals and populations. All in the hope of finding differences that can be exploited to selectively kill pathogens, or selectively kill tumors, while sparing the host.

www.agilent.com

For Research Use Only. Not for use in diagnostic procedures.

This information is subject to change without notice.

© Agilent Technologies, Inc. 2020
Published in the USA, January 23, 2020
5994-1630EN
DE.2789467593

 **Agilent**
Trusted Answers

Application Note

Cell Analysis and
Metabolomics

Extracellular Flux Analysis and ^{13}C Stable-Isotope Tracing Reveals Metabolic Changes in LPS-Stimulated Macrophages

Authors

Agnieszka Broda and Gerald Larrouy-Maumus
MRC Centre for Molecular Bacteriology and Infection,
Department of Life Sciences,
Faculty of Natural Sciences,
Imperial College London,
London, SW7 2AZ, UK

Sufyan Pandor
Agilent Technologies, Inc.
Cheshire, UK

Abstract

Eukaryotic cells are known to generate ATP by mitochondrial (oxidative phosphorylation) and non-mitochondrial (glycolysis) metabolism. Agilent Seahorse technology is an invaluable tool to gain access in real time to the bioenergetics activity of the cell by measuring cellular oxygen consumption rates (OCR) and extracellular acidification rates (ECAR) as measures of mitochondrial respiration and glycolysis, respectively. Even though Seahorse provides phenotypic information about the bioenergetic state of the cell, an in-depth understanding of the changes in the metabolic pathways requires measuring the abundances and rates of metabolite interconversion of the molecules involved in the key metabolic pathways (e.g. glycolysis, tricarboxylic acid cycle (TCA) cycle, pentose phosphates pathway). This is achieved by performing stable-isotope tracing analysis on an LC/Q-TOF, providing a detailed view of cellular metabolism. Advancements in LC/Q-TOF technology coupled with integrated qualitative flux analysis software reveal more details by tracking the *in vivo* turnover of metabolites through pathways. In this application note, we present an example of using both Seahorse XF technology and ^{13}C stable-isotope-tracing analysis with Agilent MassHunter VistaFlux software to study the response to lipopolysaccharide (LPS) treatment of RAW 264.7 macrophages. The aim of this application note is to demonstrate the complementarity of phenotypic analysis using Seahorse technology and targeted stable-isotope-tracing analysis using an Agilent 6546 LC/Q-TOF.

Introduction

Immunometabolism research has significantly expanded our understanding of immune cell function in recent years. Modulation of metabolism appears to be crucial for controlling cell fate.^{1,2} In this context, Seahorse technology enables insight into the bioenergetic state of the cell in response to stimuli. This is achieved by simultaneously measuring, in real time, the changes in oxygen consumption rate (OCR, a qualitative indicator of mitochondrial oxidative phosphorylation) and the rate of extracellular acidification (ECAR, a qualitative indicator of glycolysis), as shown in Figure 1.

To gain further insight into the mechanism leading to changes in OCR and ECAR in response to stimuli, metabolomics allows a direct snapshot of pathway activities and metabolite regulation. For yet more detailed information on metabolic pathway changes, stable-isotope-tracing analysis (e.g. ¹³C, ¹⁵N, ²H) can be applied. Stable-isotope labeling provides a different picture of intracellular metabolism than metabolomics. Although untargeted metabolomics provides the abundance of different metabolites within metabolic pathways, several metabolic changes do not *a fortiori* result in an increase or a decrease in the metabolite level. Stable-isotope-tracing provides information not revealed by conventional untargeted metabolomics by measuring the rates of metabolite interconversion as a readout of metabolic enzyme regulation. This makes stable-isotope-tracer studies a powerful option to probe metabolic changes in complex biological systems.

Insights into the full picture of cell metabolism from the combination of Seahorse and LC/Q-TOF data can inform biological research as answers from

one platform can drive experiments on the other, allowing a feedback loop for follow-up experiments (Figure 2).

Such workflows can provide accurate answers to biological questions much faster as both experiments are targeted

(specific assays on the Seahorse and pathway-driven experiments on the LC/Q-TOF).

Within immunometabolism research, macrophages are known to play a central role in pathogen recognition, exhibiting

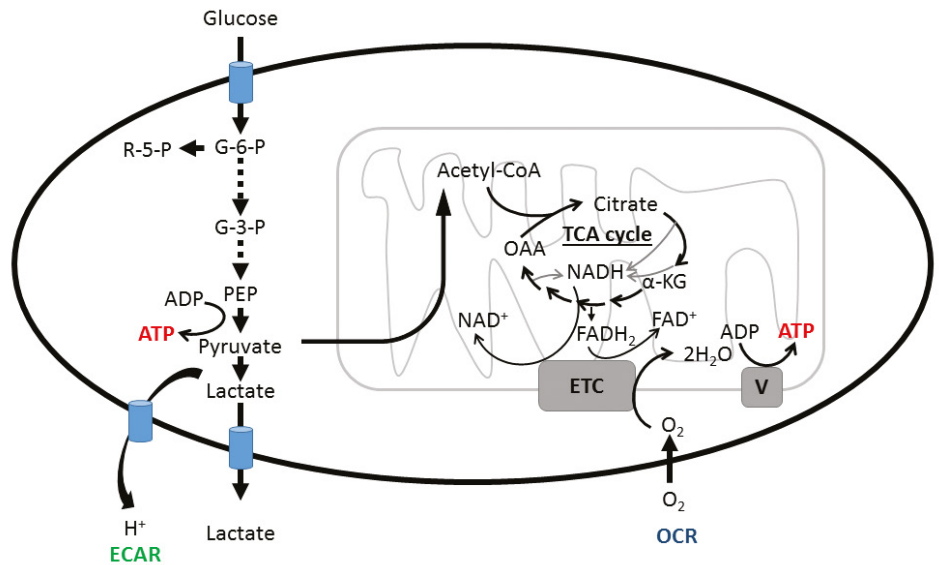


Figure 1. Schematic illustration of cellular metabolism pathways and the link between phenotypic measurements using Agilent Seahorse (ECAR and OCR) and the metabolites from relevant metabolic pathways (e.g., glycolysis, TCA cycle, and mitochondrial respiration) using stable-isotope-tracing analysis by LC/Q-TOF. G-6-P: glucose-6-phosphate; R-5-P: ribose-5-phosphate; G-3-P: glyceraldehyde-3-phosphate; PEP: phosphoenolpyruvate; ECAR: extracellular acidification rate; OCR: oxygen consumption rate; ETC: electron transport chain.

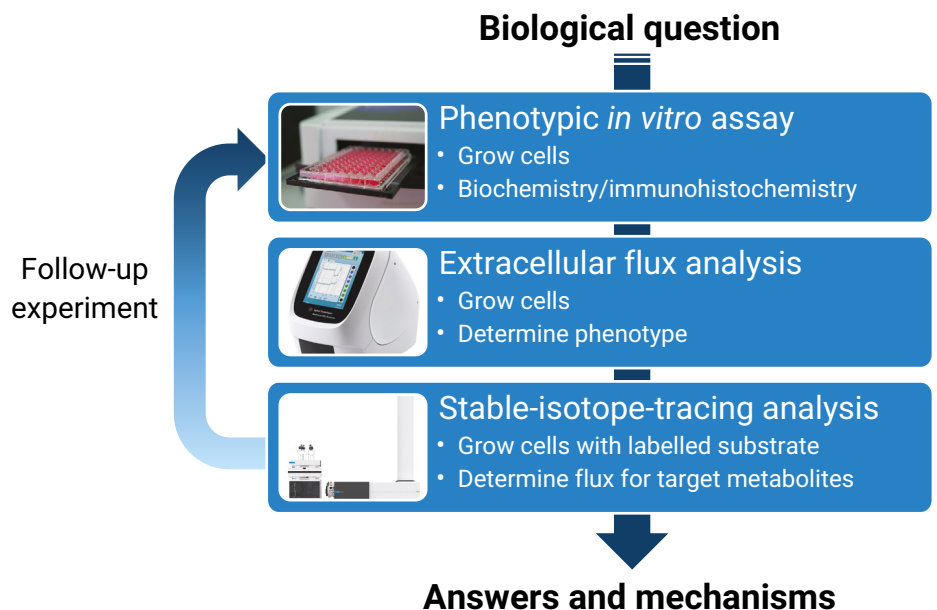


Figure 2. Workflow used to address biological questions by combining conventional phenotypic assays, Agilent Seahorse measurements, and stable-isotope-tracing analysis on an LC/Q-TOF.

an array of immediate physiological remodeling in response to pathogen stimuli. Elucidation of the mechanisms regulating metabolic pathways and the balance of metabolites is crucial for understanding macrophage function and their remodeling upon external stimuli. One such example is macrophage activation. Classical activation of macrophages is performed by pro-inflammatory stimuli such as LPS and/or interferon gamma (IFN γ). Several studies have demonstrated that activated macrophages undergo a metabolic switch that includes immediate up-regulation of glycolysis, remodeling of the TCA cycle, and the inhibition of mitochondrial respiration.³ These processes follow an orchestrated sequence of metabolic adaptations that can be followed in real time via extracellular flux analysis.¹⁰

For example, itaconic acid, a non-amino organic acid derived from *cis*-aconitate by the action of *cis*-aconitate decarboxylase (*cadA*), is known to be one of the most highly induced metabolites following LPS stimulation in bone marrow derived macrophages (BMDMs).^{4,5} This process is known to be energy costly for the macrophages as they lose the ability to perform mitochondrial substrate-level phosphorylation.⁶

In this application note, we present an example of the combination of Seahorse XF technology with ¹³C stable-isotope-tracing analysis using MassHunter VistaFlux software to

understand the response of RAW 264.7 macrophages to 4 hours of LPS treatment. The presented workflow can be adapted to different cell types to decipher the molecular mechanisms underpinning immunometabolism.

Experimental

Cell culture and reagents

RAW 264.7 cells were prepared from the frozen stock ($-80\text{ }^{\circ}\text{C}$) and cultured in a tissue culture flask ($\sim 0.5 \times 10^5$ cells/mL) in DMEM medium (Dulbecco's Modified Eagle's Medium, Sigma-Aldrich) supplemented with 10% heat-inactivated fetal bovine serum (FBS). After 48 hours of incubation at $37\text{ }^{\circ}\text{C}$ in CO_2 , confluent cells were split and cultured in fresh media. The process of splitting was repeated five to six times until the cells were fully recovered from being frozen.

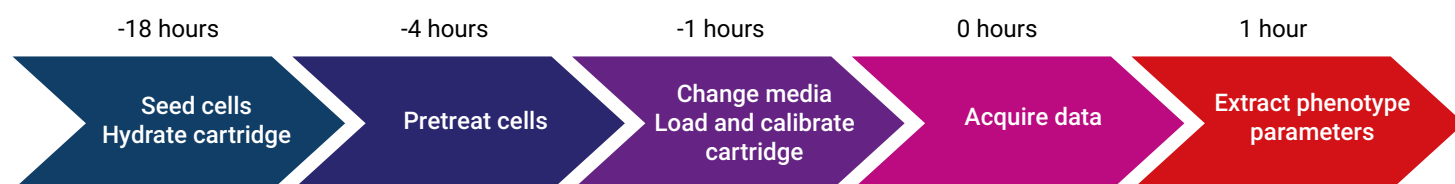
Phenotypic *in vitro* assay-cytokine measurement by ELISA

The RAW 264.7 cells were cultured in a six-well plate and incubated at $37\text{ }^{\circ}\text{C}$ in CO_2 for three to five hours to adhere, then treated with LPS at 100 ng/mL final or plain media for the next four hours. The supernatant was collected for cytokine TNF α analysis. The TNF α production by RAW 264.7 macrophages was determined using the mouse TNF α ELISA kit (Ready-SET-Go; Affymetrix eBioscience; Invitrogen 88732486) according to the manufacturer's instructions. Absorbance readings were measured at 450 nm.

Extracellular flux analysis on the Seahorse XFp Analyzer

RAW 264.7 cells were seeded on an eight-well miniplate at cell densities of 4×10^5 cells/mL and left to adhere overnight. Cells were or were not treated with LPS at 100 ng/mL final or plain media, and after four hours, the OCR and ECAR were measured using an Agilent Seahorse XFp Analyzer. The day before the assay, the sensor cartridge was hydrated by filling the utility plate's moats and wells with 400 and 200 μL of double-distilled sterile water, respectively, and incubating overnight at $37\text{ }^{\circ}\text{C}$ in a non- CO_2 incubator. On the day of the assay, the water was replaced with 200 μL of prewarmed Agilent XF calibrant and incubated for another one hour. Also, the culture medium was replaced with 180 μL of Agilent Seahorse XF RPMI medium, pH 7.4, that was supplemented with 10 mM glucose, 2 mM sodium pyruvate, and 2 mM glutamine, and the cells were incubated at $37\text{ }^{\circ}\text{C}$ in a non- CO_2 incubator for one hour. The Seahorse miniplate with cells was placed into the XFp Analyzer for subsequent analysis at $37\text{ }^{\circ}\text{C}$. Measurement cycles consisted of three minutes mixing and three minutes measuring. Baseline rates were measured at $37\text{ }^{\circ}\text{C}$ three times before sequentially injecting the following mitochondrial inhibitors: oligomycin (2 μM), carbonyl cyanide *p*-(trifluoromethoxy) phenylhydrazone (FCCP, 2 μM), and a rotenone/antimycin A mixture (0.5 μM) all from the Agilent Seahorse XFp Cell Mito Stress Test kit. After the addition of each inhibitor, three readings were taken. OCR and ECAR

Seahorse XFp Analyzer workflow



were automatically calculated by the Seahorse XFP Wave software. Each data point represents an average of three different well measurements that were normalized to the number of cells per well. For a more complete understanding of the general metabolic changes, a phenotype analysis was conducted using the Cell Mito Stress Test data result file.

Qualitative flux analysis

Metabolite extraction

RAW 264.7 cells were seeded on a six-well plate at a cell density of 5×10^5 cells/mL and incubated for three to five hours to adhere. After this time, the media was changed for the media supplemented with [U- $^{13}\text{C}_6$]-glucose at 4.5 mg/mL. Cells were or were not treated with LPS at 100 ng/mL media concentration and in the presence of [U- $^{13}\text{C}_6$]-glucose at a concentration equivalent to a 1:1 ratio of ^{12}C and ^{13}C glucose present in the culture medium, then incubated for four hours. The microplate was placed on ice, and the media was removed carefully. The adhered cells were washed three times with cold PBS before addition of a metabolite extraction buffer (acetonitrile, methanol, and water at a ratio of 40:40:20 v/v/v at -20°C) at a density of 10^7 cells/mL. Cells were then scraped and transferred to an Eppendorf vial. A 100 μL aliquot of the metabolite solution was then mixed with 100 μL of acetonitrile with 0.2% acetic acid at -20°C and centrifuged for 10 minutes at 17,000 g at 4°C . The final concentration of 70% acetonitrile was compatible with the starting conditions of the HILIC chromatography. The supernatant was then transferred to an Agilent LC/MS V-shape vial (p/n 5188-2788) and 4 μL was injected into the LC/MS.

LC/Q-TOF data acquisition

Data were acquired on an Agilent 1290 Infinity II LC coupled to an 6546 LC/Q-TOF system. Chromatographic separation was performed on an Agilent InfinityLab Poroshell 120 HILIC-Z, 2.1×100 mm, $2.7 \mu\text{m}$ column (part number 675775-924). The HILIC methodology was optimized for polar acidic metabolites (details in Table 1). For easy and consistent mobile phase preparation, a concentrated 10x solution consisting of 100 mM ammonium acetate, pH 9.0, in water was prepared to produce mobile phases A and B.

Target metabolite list creation

As Seahorse provides phenotypic information about glycolysis (ECAR) and mitochondrial oxidative phosphorylation (OCR), a target list of metabolites related to those pathways was created using Agilent MassHunter Pathways to PCDL software. From a public pathways database, the software generates a target personal compound database (PCDL) that contains names, formulas, and various identifiers. Addition of metabolite retention times in the target PCDL were provided from a pre-existing in-house database.

Table 1. Liquid chromatography conditions.

LC Conditions			
Column	Agilent InfinityLab Poroshell 120 HILIC-Z, 2.1×100 mm, $2.7 \mu\text{m}$ (p/n 675775-924)		
Mobile Phase	A) 10 mM ammonium acetate in water, pH 9 with $5 \mu\text{m}$ Agilent InfinityLab Deactivator Additive (p/n 5191-4506) B) 10 mM ammonium acetate, pH 9 in 10:90 (v:v) water/acetonitrile		
Flow Rate	0.5 mL/min		
Gradient	Time (min)	%A	%B
	0	0	100
	11.5	30	70
	12	0	100
	15	0	100
	20	Post time	
Column Temperature	30°C		
Injection Volume	1 μL		
Multisampler Temperature	6°C		

Table 2. Mass spectrometry conditions.

MS Conditions	
MS System	Agilent 6546 LC/Q-TOF
SWARM Autotune Selection	m/z 50 to 750 fragile ion mode
Ionization Source	Agilent Jet Stream
Polarity	Negative
Gas Temperature	200°C
Drying Gas Flow	10 L/min
Nebulizer Pressure	40 psig
Sheath Gas Temperature	300°C
Sheath Gas Flow	12 L/min
Capillary Voltage	3000 V
Nozzle Voltage	0 V
Fragmentor	115
Acquisition Range	m/z 40–1000
Reference Mass	m/z 68.995758 and 980.016375

Batch isotopologue data analysis

Agilent MassHunter Profinder 10 is the batch-processing module of VistaFlux. Data files were imported and assigned to treatment groups. The chromatographic data were time-aligned against an in-house database of compounds with known retention times. The batch isotopologue extraction wizard was used to extract isotopologues for the target metabolites list as well as to correct for natural abundance of ^{13}C and for the tracer purity. In stable-isotope tracing, results are self-normalized for each metabolite as the isotopologue enrichment percentage is calculated relative to the other isotopologues. The ^{13}C tracer purity in this experiment was 50%, so the result of these corrections is that 100% label incorporation represents full incorporation of ^{13}C into the metabolite. The results from Profinder were transferred to Omix Premium, another module of VistaFlux, for visualization of metabolic fluxes on pathways.

Statistical analysis

Data are presented as the mean \pm standard error of the mean from two biological replicates and four technical replicates per condition for all experiments. Unpaired two-tailed Student's t-tests were used to compare values, with $p < 0.05$ considered significant.

Results and discussion

LPS stimulation induces a large increase in TNF α

RAW 264.7 cells are widely used to understand molecular mechanisms of macrophage activation. Here, we assessed macrophage activation by measuring the amount of tumor necrosis factor alpha (TNF α) released in the cell culture medium in response to LPS stimulation. As expected, activation of

VistaFlux workflow



RAW 264.7 cells by 100 ng/mL of LPS for four hours leads to a 100-fold increase in the abundance of secreted TNF α , confirming the activation state of the cells (Figure 3).

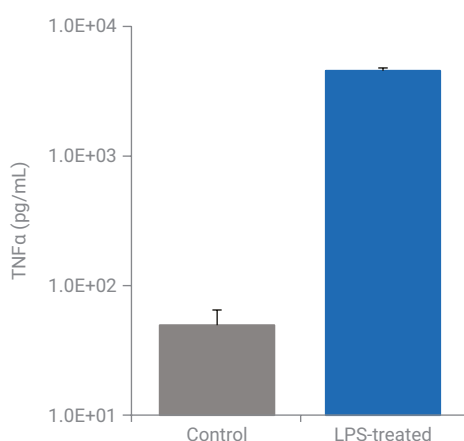


Figure 3. Level of TNF α in response to four hours of stimulation by 100 ng/mL of LPS in RAW 264.7 cells.

LPS stimulation induces a shift towards a glycolytic phenotype

To demonstrate how LPS activation impacts cell bioenergetics in RAW 264.7, we investigated the cell phenotype with the Seahorse XFp Analyzer (Figure 4). The Seahorse phenotype analysis software shows the metabolic activity of cells under basal conditions and under stressed conditions to reveal the metabolic potential. The analysis showed a general shift of the RAW 264.7 towards a more glycolytic phenotype when stimulated with LPS in the basal as well as in the stressed phenotype. This is in line with the literature showing that a glycolytic switch is an essential component of the pro-inflammatory function of macrophages.⁷⁻⁹

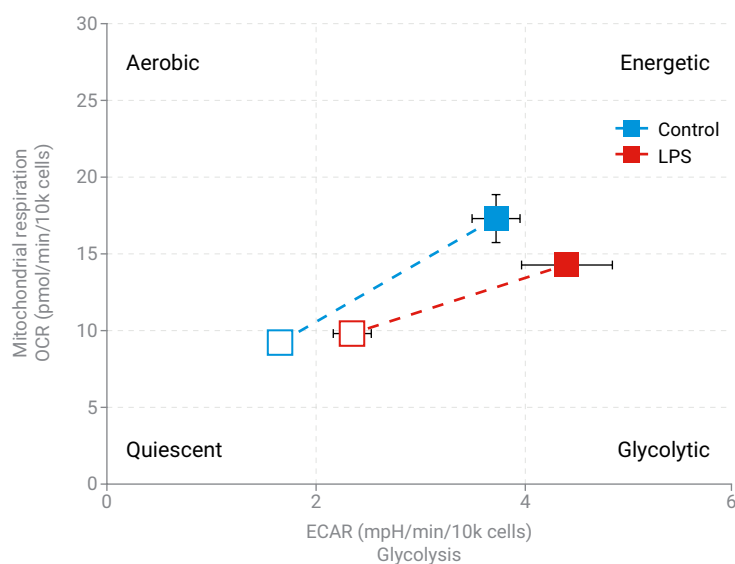


Figure 4. OCR versus ECAR plot for metabolic phenotype analysis measured in triplicates. Open quadrats represent the basal phenotype and closed quadrats the stressed phenotype (metabolic capacity after injection of oligomycin and FCCP). Four hours of stimulation by 100 ng/mL of LPS in RAW 264.7 cells induce a shift towards increased glycolytic activity.

LPS stimulation results in a redirection of carbon flux towards itaconic acid synthesis

As shown previously by Seahorse XFp analysis, LPS stimulation of RAW 264.7 cells increases ECAR. As discussed earlier, ECAR informs on glycolysis. Therefore, to gain insight into the changes in metabolite turnover in response to LPS stimuli leading to changes in ECAR, we undertook [U-¹³C₆]-glucose stable-isotope tracing focusing on metabolites involved in central carbon catabolism and the TCA cycle (Table 3). RAW 264.7 cells were simulated or not with LPS for four hours in a culture medium containing [U-¹³C₆]-glucose, and incorporation of ¹³C was determined by LC/MS.

As shown in Figure 5, both lactate and pyruvate display very high levels of ¹³C incorporation, reaching up to 95% labeled independently of the treatment applied. However, the major change occurs at the level of *cis*-aconitate, and specifically itaconic acid, where LPS activation drastically alters the isotopologue distribution. Effectively, upon LPS stimulation, a large increase in ¹³C incorporation is observed for M+1, M+2, M+4, and M+5 concomitant with a decrease in M+0. This is consistent with the literature where LPS activation is known to promote the production

of itaconic acid.^{4,5} Based on the XF data presented here, LPS stimulation leads to an increase in glycolysis. We therefore investigated the change in the isotopologue distribution of metabolites involved in this pathway. As shown in Figure 5, we observed an increase in ¹³C incorporation in metabolites involved in glycolysis as well as the oxidative branch of the TCA cycle leading towards the production of itaconic acid. An

associated decrease in metabolites found in the reductive branch of the TCA cycle was observed, confirming an inhibition of the turnover of metabolites from the reductive branch of the TCA cycle upon LPS stimulation. Taken together, these data suggest that upon LPS stimulation, RAW 264.7 cells redirect their carbon flux towards itaconic acid production, leading to an alteration in ¹³C turnover in the TCA cycle.

Table 3. Target metabolite list for isotopologue extraction showing mean measured retention time of eight control samples.

Information Pathway	Metabolite	Formula	RT (min)	CAS
ECAR	β-D-Glucose 6-phosphate	C ₆ H ₁₃ O ₉ P	9.60	15209-12-8
	D-Fructose 6-phosphate	C ₆ H ₁₃ O ₉ P	8.22	643-13-0
	β-D-Fructose 1,6-bisphosphate	C ₆ H ₁₄ O ₁₂ P ₂	10.2	488-69-7
	D-Glyceraldehyde 3-phosphate	C ₃ H ₇ O ₆ P	7.03	591-57-1
	Dihydroxyacetone phosphate	C ₃ H ₇ O ₆ P	7.95	57-04-5
	Pyruvic acid	C ₃ H ₄ O ₄	1.40	127-17-4
	Lactic acid	C ₃ H ₆ O ₃	2.21	50-21-5
OCR	Citric acid	C ₆ H ₈ O ₇	8.88	77-92-9
	<i>cis</i> -Aconitic acid	C ₆ H ₈ O ₆	7.86	585-84-2
	<i>D-threo</i> -Isocitric acid	C ₆ H ₈ O ₇	6.94	6061-97-8
	Oxoglutaric acid	C ₅ H ₆ O ₅	6.04	328-50-7
	L-Glutamate	C ₅ H ₉ NO ₄	6.25	56-86-0
	Succinic acid	C ₄ H ₆ O ₄	6.54	110-15-6
	Fumaric acid	C ₄ H ₄ O ₄	6.88	110-17-8
	L-Malic acid	C ₄ H ₆ O ₅	6.79	97-67-6
	L-Aspartic acid	C ₄ H ₇ NO ₄	1.22	56-84-8
	Itaconic acid	C ₅ H ₆ O ₄	6.68	97-65-4

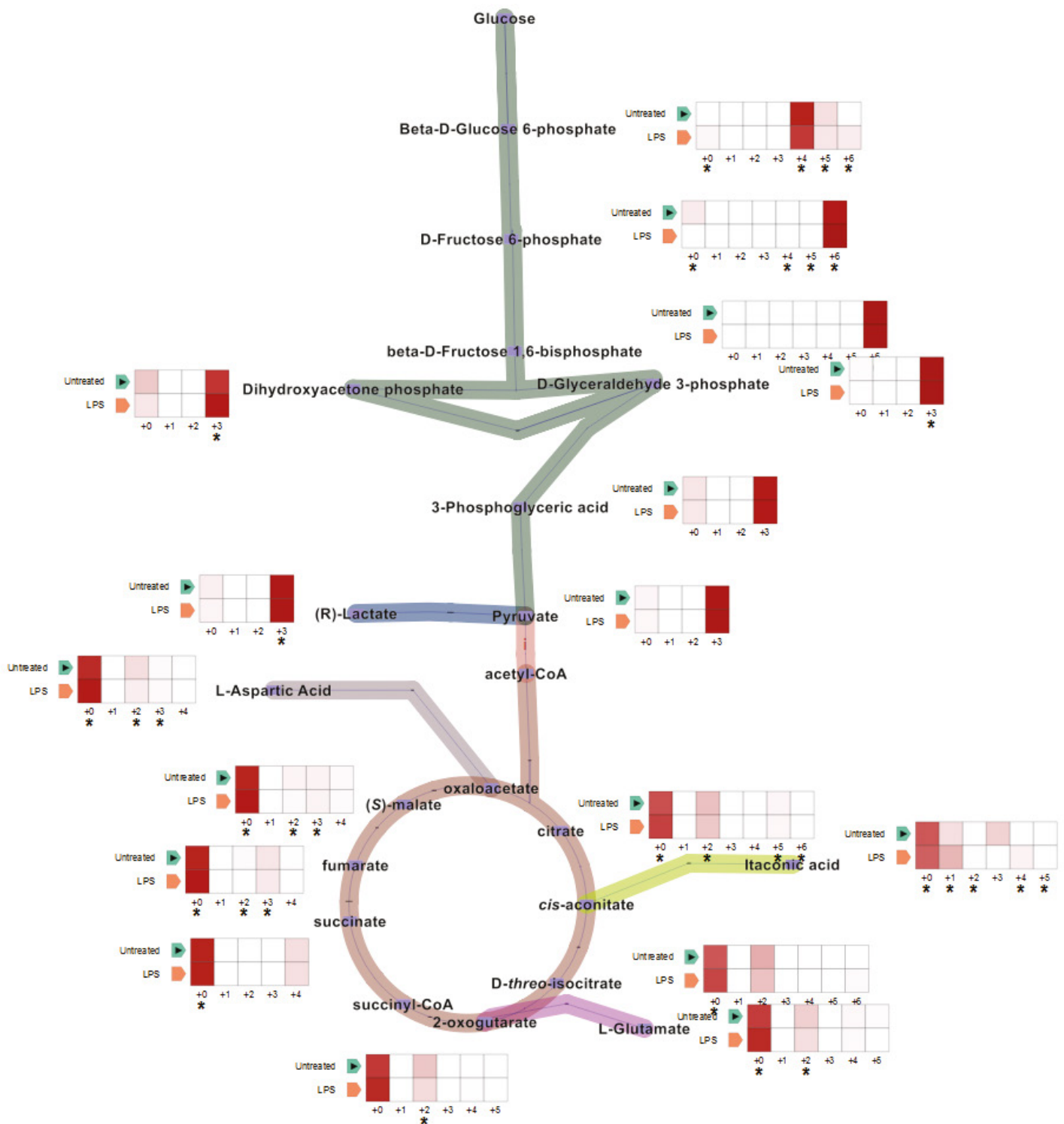


Figure 5. Summary of $[U-^{13}C_6]$ -glucose stable-isotope-tracing analysis of RAW 264.7 cells stimulated for four hours by 100 ng/mL of LPS compared to untreated RAW 264.7 cells (control). Results are displayed as quilt plots on the pathways where each quilt plot shows corrected abundance for each isotopologue for control and treated cells. Statistical significance is denoted by an *.

Conclusion

Combining real-time extracellular flux information with ¹³C stable-isotope-tracing allows greater insight into the mechanism of macrophage activation. Where Seahorse technology provides information about the metabolic phenotypes and the activities of the two major energy pathways from a macroscopic view, ¹³C stable-isotope-tracing analysis allows a microscopic insight into the pathways leading to these changes.

Seahorse XF assays provide real-time, live-cell metabolic analysis. With this technology, a glycolytic shift in the phenotype of the living macrophages was shown, which is a prerequisite for pro-inflammatory macrophage activation. This was confirmed when looking into the metabolic details by qualitative flux analysis. The increased glycolytic rate was confirmed by the increased incorporation of ¹³C into glycolysis metabolites relative to the basal case. Flux analysis also showed an increased production of itaconic acid, a potent antimicrobial compound produced by pro-inflammatory macrophages, and thereby provided a more detailed picture of the changes in metabolism.

This workflow and the technologies used can be applied to other cell types to study cell metabolism at the phenotype and metabolite levels to uncover molecular mechanisms of cell metabolism in response to external triggers or genetic manipulations.

References

1. O'Neill, L. A.; Kishton, R. J.; Rathmell, J. A Guide to Immunometabolism for Immunologists. *Nat. Rev. Immunol.* **2016**, *16*, 553–65.
2. Loftus, R. M.; Finlay, D. K. Immunometabolism: Cellular Metabolism Turns Immune Regulator. *J. Biol. Chem.* **2016**, *291*, 1–10.
3. Kelly, B.; O'Neill, L. A. Metabolic Reprogramming in Macrophages and Dendritic Cells in Innate Immunity. *Cell Res.* **2015**, *25*, 771–84.
4. Lampropoulou, V. *et al.* Itaconate Links Inhibition of Succinate Dehydrogenase with Macrophage Metabolic Remodeling and Regulation of Inflammation. *Cell Metab.* **2016**, *24*, 158–66.
5. Mills, E. L. *et al.* Itaconate is an Anti-Inflammatory Metabolite that Activates Nrf2 via Alkylation of KEAP1. *Nature* **2018**, *556*, 113–117.
6. Nemeth, B. *et al.* Abolition of mitochondrial substrate-level phosphorylation by itaconic acid produced by LPS-induced Irg1 expression in cells of murine macrophage lineage. *FASEB J* **2016**, *30*, 286–300.
7. Van den Bossche, J. *et al.* Mitochondrial Dysfunction Prevents Repolarization of Inflammatory Macrophages. *Cell Rep.* **2016**, *17*, 684–696.
8. Van den Bossche, J.; Baardman, J.; de Winther, M. P. Metabolic Characterization of Polarized M1 and M2 Bone Marrow-Derived Macrophages Using Real-time Extracellular Flux Analysis. *J. Vis. Exp.* **2015**, doi:10.3791/53424.
9. Artyomov, M. N.; Sergushichev, A.; Schilling, J. D. Integrating Immunometabolism and Macrophage Diversity. *Semin. Immunol.* **2016**, *28*, 417–424.
10. Kam, Y. *et al.* Real Time Discrimination of Inflammatory Macrophage Activation Using Agilent Seahorse XF Technology. *Agilent Technologies application note*, publication number 5991-8342EN, **2018**.

www.agilent.com/chem

For Research Use Only. Not for use in diagnostic procedures.

DE.5524421296

This information is subject to change without notice.

© Agilent Technologies, Inc. 2020
Printed in the USA, April 14, 2020
5994-1846EN

 **Agilent**
Trusted Answers

Application Note

Lipidomics



Improving Coverage of the Plasma Lipidome Using Iterative MS/MS Data Acquisition Combined with Lipid Annotator Software and 6546 LC/Q-TOF

Authors

Jeremy Koelmel
Department of Chemistry,
University of Florida,
Gainesville, FL, USA

Mark Sartain, Juli Salcedo,
Adithya Murali, Xiangdong Li,
and Sarah Stow
Agilent Technologies, Inc.
Santa Clara, CA, USA

Introduction

A major challenge in mass spectrometry-based lipidomics is the comprehensive characterization of a large and diverse set of lipid species, spanning a wide concentration range within a biological sample. While shotgun lipidomics has advanced the field of lipid analysis, it suffers from limitations including the failure to distinguish isobaric species, which may be of biological importance and reduced dynamic range due to ionization suppression. This led to chromatography-based lipid profiling approaches using high-performance liquid chromatography (HPLC) coupled to high resolution mass spectrometry (MS).

To enable product-ion spectral matching against *in silico* generated databases, confident lipid annotation requires data acquisition at the MS/MS level. However, while LC separation helps elucidate isomeric lipid species and reduce complexity, data-dependent high-resolution MS/MS data are limited by the number of precursors that can be selected for fragmentation during chromatographic elution. Therefore, it is not possible to acquire all the MS/MS spectra of interest in a single analysis for complex samples. Due to concentration bias, this strategy often misses important lipid species of low abundance.

This Application Note demonstrates solutions to these challenges. We used reversed-phase (RP) chromatography, which is well suited to resolve many cases of isomeric lipids, and is a popular choice for profiling plasma¹, tissue², and cellular lipids in a comprehensive manner. We coupled this LC separation to the Agilent 6546 LC/Q-TOF, a mass spectrometer designed to provide wide dynamic range while simultaneously providing improved resolution independent of acquisition speed. We also evaluated the fully automated Q-TOF Iterative MS/MS acquisition mode, in which a sample is injected multiple times, and precursors previously selected for MS/MS fragmentation are excluded on a rolling basis. These results demonstrate that plasma lipidome coverage can be significantly improved with Iterative MS/MS. Iterative MS/MS data can be used by Agilent Lipid Annotator software as part of a comprehensive lipidomics workflow.

Experimental

Reagents and chemicals

All reagents and solvents were HPLC or LC/MS grade. Acetonitrile, methanol, and isopropanol were purchased from Honeywell (Morristown, NJ, USA). Ultrapure water was produced with a Milli-Q Integral system equipped with a LC-Pak Polisher and a 0.22 µm point-of-use membrane filter cartridge (EMD Millipore, Billerica, MA, USA). Ammonium fluoride and LC/MS grade ammonium acetate were purchased from Millipore Sigma (St. Louis, MO, USA). NIST SRM 1950 human plasma was purchased from Millipore Sigma.

Sample preparation

NIST SRM 1950 plasma was thawed on ice, and plasma lipids were extracted with a modified Folch extraction procedure. Methanol (400 µL) was added to a 50 µL aliquot of thawed plasma in a 2 mL Eppendorf tube, vortexed briefly, then bath-sonicated for five minutes. Chloroform (800 µL) was added, and vortexed for one minute. To induce phase partitioning, 240 µL of water was added. The mixture was then vortexed for one minute, and centrifuged at 16,000 × g for two minutes at 4 °C. The lower layer was carefully removed with a gas-tight glass syringe, and transferred to a 2 mL Agilent A-Line amber glass vial. To re-extract the remaining interphase and upper phase layers, 900 µL chloroform/methanol/water (86:14:1) was added, and the mixture was vortexed for one minute and centrifuged again. The combined lower layers from the two 50 µL extractions were combined and dried by a vacuum concentrator. Dried lipid extracts were reconstituted with 100 µL of a methanol/chloroform mixture (9:1, v/v), vortexed for one minute, and taken to deactivated 250 µL autosampler glass inserts before LC/MS analysis. For positive mode analysis, synthetic rubber

septa (p/n 5181-1212) were used, and 2 µL injections were made. For negative mode analysis, PTFE/Silicone/PTFE septa (p/n 5185-5861) were used, and 5 µL injections were made.

Instrumentation

LC system

Agilent 1290 Infinity II LC including:

- Agilent 1290 Infinity II High Speed Pump (G7120A)
- Agilent 1290 Infinity II Vialsampler with thermostat (G7129B)
- Agilent 1290 Infinity II Multicolumn Thermostat (G7116B)

MS system

Agilent 6546 LC/Q-TOF with an Agilent Jet Stream Technology source

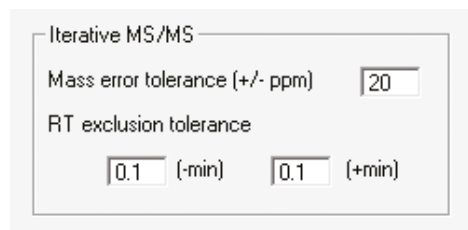
Method

Data were acquired either using a conventional AutoMS/MS method or an Iterative MS/MS method, as indicated. Tables 1 and 2 provide the chromatography and 6546 Q-TOF conditions and parameters.

Table 1. Chromatographic conditions.

Parameter	Agilent 1290 Infinity II LC	
Analytical Column	Agilent InfinityLab Poroshell 120 EC-C18, 3.0 × 100 mm, 2.7 µm (p/n 695975-302)	
Guard Column	Agilent InfinityLab Poroshell 120 EC-C18, 3.0 × 5 mm, 2.7 µm (p/n 823750-911)	
Column Temperature	50 °C	
Injection Volume	2 µL (positive), 5 µL (negative)	
Autosampler Temperature	4 °C	
Needle Wash	15 seconds in wash port (50:50 methanol/isopropanol)	
Mobile Phase	A) 10 mM ammonium acetate, 0.2 mM ammonium fluoride in 9:1 water/methanol B) 10 mM ammonium acetate, 0.2 mM ammonium fluoride in 2:3:5 acetonitrile/methanol/isopropanol	
Flow Rate	0.6 mL/min	
Gradient Program	Time (min)	%B
	0.00	70
	1.00	70
	3.50	86
	10.00	86
	11.00	100
	17.00	100
	17.10	70
	19.00	70
Stop Time	19 minutes	
Post Time	None	
Observed Column Pressure	170 to 330 bar	

Iterative MS/MS parameters in the Acquisition method editor were set up as follows:



To invoke Iterative M/MS, the Acquisition worklist was set up as follows:

- Right-click, and select **Add Columns**.
- Select **Iterative** from available columns under **MS Parameter** Column Type (Figure 1).
- Typing **Start** or **Reset** in the Iterative column (Figure 2) indicates the beginning of an iteration set. This resets any prior rolling exclusion list, and begins a new exclusion list.
- Typing **Iterative** or any other word is used to specify the subsequent iterative injections that both use and add to the exclusion list.
- A blank cell indicates the injection neither uses nor adds to the exclusion list, but does not reset the worklist. However, note that a full or partial (time segment) Targeted MS/MS or Scan (MS only) acquisition method will reset the rolling exclusion list.

Inj Vol (µl)	Iterative	Comment
As Method	start	
As Method	iterative	
As Method		

Figure 2. Worklist setup for Iterative MS/MS.

Table 2. 6546 Q-TOF AutoMS/MS parameters.

Parameter	6546 LC/Q-TOF
Gas Temperature	200 °C
Gas Flow	10 L/min
Nebulizer (psig)	50
Sheath Gas Temperature	300 °C
Sheath Gas Flow	12 L/min
VCap	3,500 V (+), 3,000 V (-)
Nozzle Voltage	0 V
Fragmentor	150 V
Skimmer	65 V
Octopole RF Vpp	750 V
Reference Mass	m/z 121.050873, m/z 1221.990637 (+) m/z 119.03632, m/z 980.016375 (-)
MS and MS/MS Range	m/z 40–1700 (+)
Min MS and MS/MS Acquisition Rate	3 spectra/s
Isolation Width	Narrow (~ 1.3 m/z)
Collision Energy	20 eV (+), 25 eV (-)
Max Precursors Per Cycle	3
Precursor Abundance-Based Scan Speed	Yes, target 25,000 counts/spectrum
Use MS/MS Accumulation Time Limit	Yes
Reject Precursors That Cannot Reach Target TIC	No
Threshold for MS/MS	5,000 counts and 0.001%
Active Exclusion Enabled	Yes, one repeat, then exclude for 0.05 minutes
Purity	Stringency 70 %, cut off 0 %
Isotope Model	Common organic molecules
Sort Precursors	1, 2, unknown
Static Exclusion Ranges	m/z 40 to 151 (+) m/z 40 to 210 (-)

Add Columns

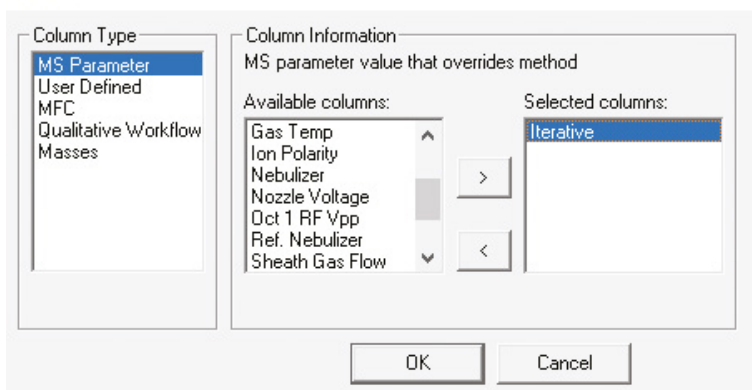


Figure 1. The Add Columns dialog box.

Software

Agilent MassHunter Q-TOF Data Acquisition Version 10 was used to operate the 6546 LC/Q-TOF system. Agilent MassHunter Lipid Annotator Version 1.0 was used for all other data analyses. Default method parameters were used, except only $[M+H]^+$ and $[M+NH_4]^+$ precursors were considered for positive ion mode analysis, and only $[M-H]^-$ and $[M+HAc-H]^-$ precursors were considered for negative ion mode analysis. Agilent MassHunter PCDL Manager Version B.08 SP1 was used to manage and edit the exported annotations.

Results and discussion

Lipid Annotator software analysis of plasma Iterative MS/MS data

Confident lipid annotation requires data acquisition at the MS/MS level to enable product ion spectral matching against *in silico*-generated databases. This study used a novel software tool (Lipid Annotator) with a combination of Bayesian scoring, a probability density algorithm, and non-negative least squares fit to search a theoretical lipid library (modified LipidBlast) developed by Kind; *et al.*^{3,4} to annotate the MS/MS spectra. Lipid Annotator takes special care not to over-annotate lipid entities by only providing the level of structural information confidently informed by the MS/MS spectra.

Previously, a Q-TOF Iterative MS/MS acquisition mode was shown to be effective for in-depth peptide mapping of monoclonal antibodies⁵. We applied this mode of Iterative Acquisition on the 6546 LC/Q-TOF to a complex lipid sample. Figure 3 illustrates the strategy of Iterative MS/MS. The first injection is performed as a traditional data-dependent (conventional)

Auto MS/MS analysis, where the top N most abundant precursors are selected for fragmentation in consideration of an active exclusion list. In subsequent injections, precursors selected for MS/MS fragmentation in the previous injections are excluded on a rolling basis with customizable mass error tolerance and retention time exclusion tolerance.

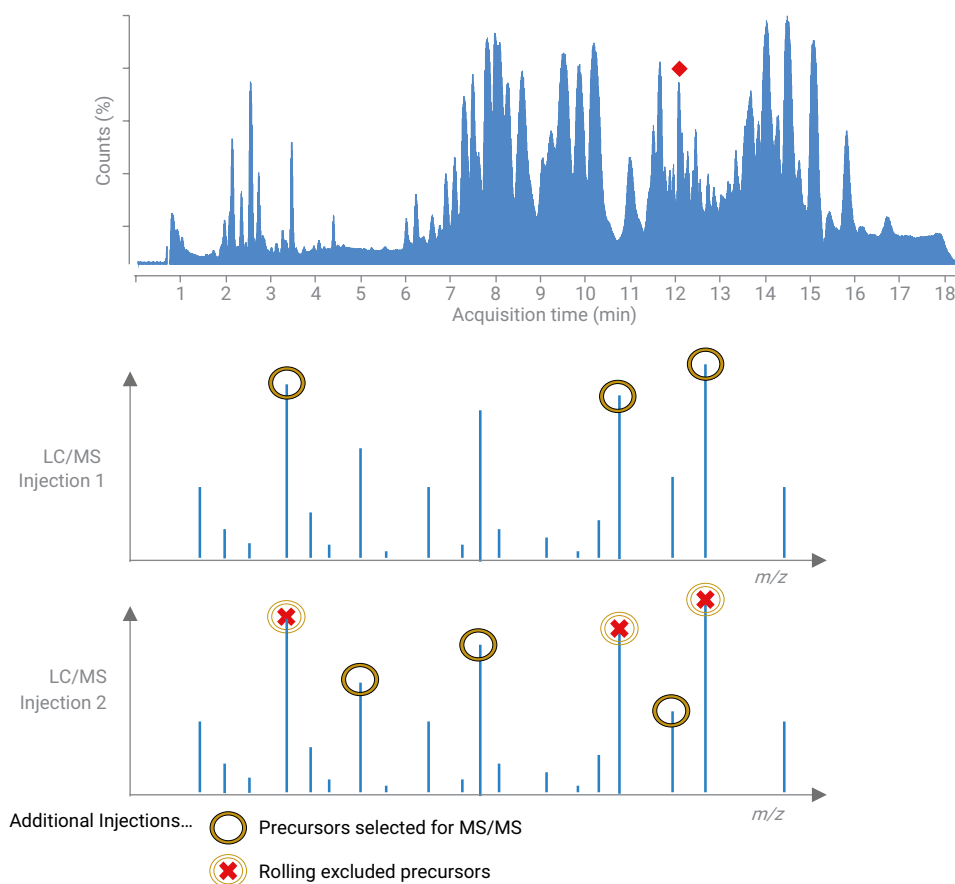
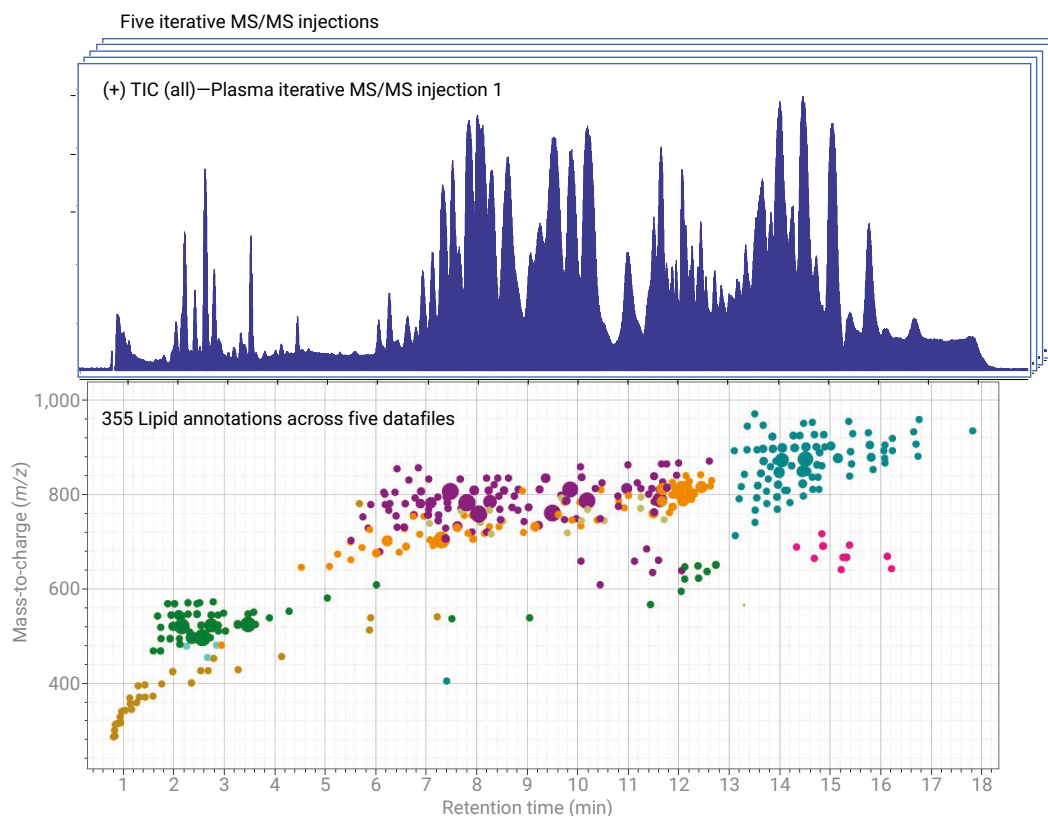


Figure 3. Principle of Iterative MS/MS.

Lipid Annotator provides the ability to analyze multiple MS/MS data files from the same sample origin together as a batch. Figure 4 illustrates an analysis of five plasma Iterative MS/MS data files.

There were 355 specific lipids (including isomers with different RTs) representing 14 classes annotated across the five positive ion mode data files. Separately, a batch of five negative ion mode Iterative

MS/MS data files was analyzed, resulting in 326 specific lipids representing 20 lipid classes (not shown).



Lipid classes
Number of lipids per class

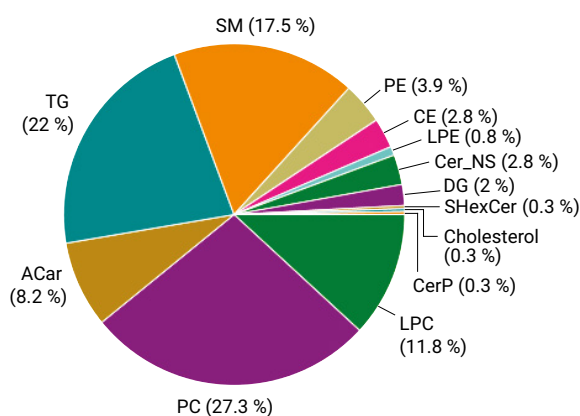


Figure 4. Typical total ion chromatogram (TIC) of plasma in positive ion mode aligned with view of Lipid Annotator software. Results shown are the combined analysis of five Iterative MS/MS data files. Annotated lipid features are plotted as *m/z* versus retention time, and colored by lipid class corresponding to the pie chart, where the numbers of annotated lipids are shown as percentages.

Iterative MS/MS increases lipid annotations

The number of cumulative lipid annotations in plasma across multiple Iterative MS/MS data acquisition files increased compared to conventional AutoMS/MS files (Figure 5). These results suggest that 3 to 5 Iterative MS/MS injections are sufficient for comprehensive lipid annotation in plasma with the method parameters used in this study. While plasma represents a common and complex biological sample, it is important to note that the optimal number of injections may depend on sample complexity and LC/MS acquisition method parameters. For plasma extracts in positive mode, applying Iterative MS/MS to five sequential injections increased the coverage of unique annotated lipids by 69 % (n = 355) compared with conventional AutoMS/MS acquisition (n = 223) across five sequential injections (Figure 5A). Likewise, in negative mode analysis of plasma, 34 % more lipid annotations were obtained with five injections of Iterative MS/MS (n = 326) compared to conventional MS/MS (n = 243) (Figure 5B). Taken together, these results show that due to the spectral density of numerous lipid precursors in a chromatographic run, especially in positive ion mode, a substantial benefit is obtained using Iterative MS/MS for LC/MS/MS-based lipidomics data acquisition.

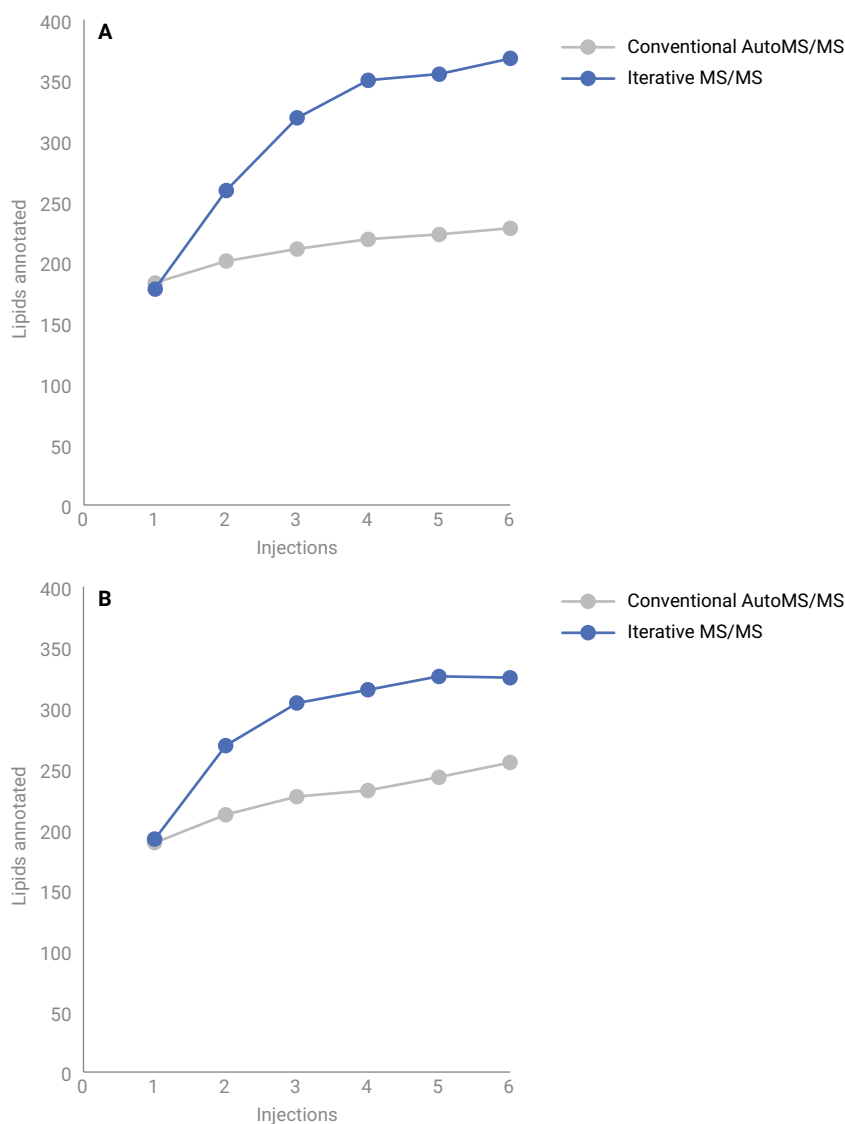


Figure 5. Cumulative unique annotated lipid features from Lipid Annotator software across multiple data acquisition files for positive (A) and negative (B) ionization modes.

Iterative MS/MS enriches lipid ions of low abundance and specific lipid classes

In agreement with the sequential exclusion of highly abundant lipid precursors in Iterative MS/MS mode, we observed that the mean peak abundance of triggered lipid precursors decreased across the first three injections of plasma in both positive (Figure 6A) and negative (Figure 6B) polarity datasets. Additionally, the peak abundances of annotated lipids in the second injection were significantly lower than the initial injection for both positive and negative polarity datasets (t-test p-value <0.001).

Due to the iterative exclusion of abundant precursors, we observed that Iterative MS/MS enriched lipid classes that were of low abundance (for example, diacylglycerols), ionized less efficiently (for example, free cholesterol), or located in spectral-dense regions of the chromatogram (for example, triacylglycerols). Table 3 shows examples of lipid classes that were highly enriched with sequential injections of Iterative MS/MS compared to conventional AutoMS/MS.

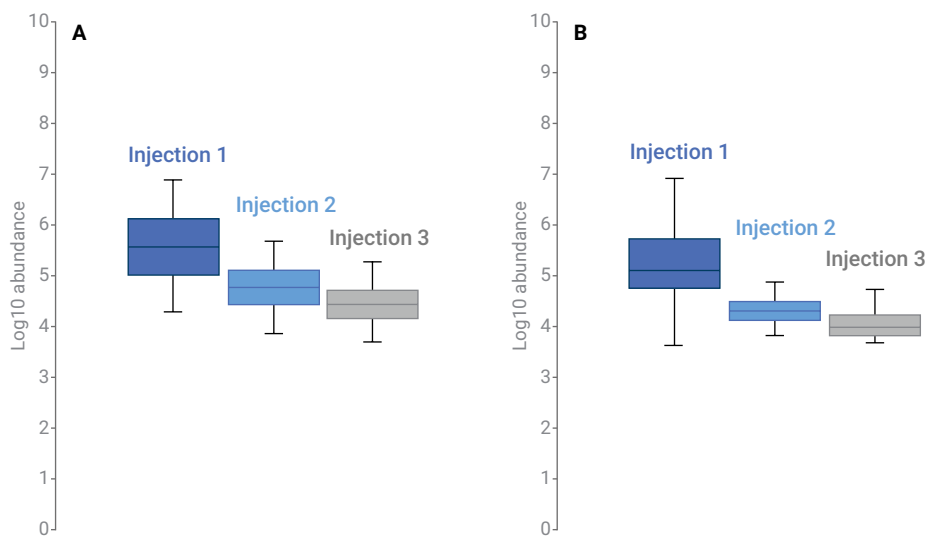


Figure 6. Box plots of feature abundances corresponding to annotated lipids from three sequential Iterative MS/MS injections in positive (A) and negative (B) ionization modes.

Table 3. Lipid classes highly enriched with Iterative MS/MS. Numbers of cumulative annotated lipids are provided for five sequential injections acquired with conventional AutoMS/MS compared to Iterative MS/MS data acquisition.

Lipid Class (polarity)	Number of Annotations AutoMS/MS	Number of Annotations Iterative MS/MS
Ceramide Nonhydroxy Fatty Acid-Sphingosines (+)	2	10
Cholesterol Esters (+)	4	10
Free Cholesterol (+)	0	1
Diacylglycerols (+)	1	7
Phosphatidylethanolamines (+)	2	14
Triacylglycerols (+)	46	78
Ether-linked phosphatidylcholines (-)	17	28
Lysophosphatidylinositols (-)	5	9
Phosphatidylethanolamines (-)	9	20

Figure 7 further demonstrates a specific example of lipid class enrichment, where precursors corresponding to cholesterol esters of low abundance were selected for MS/MS fragmentation in sequential injections.

MS/MS acquisition parameter optimization with consideration of lipid isomers

To ensure optimal coverage of plasma lipids, MS/MS acquisition method parameters were found to be critical. As a first step, Lipid Annotator uses a feature-finding algorithm on the AutoMS/MS or Iterative MS/MS data file. Feature finding is performed at the MS1 level, and MS/MS spectra are associated with each feature in a subsequent step. Only features with associated MS/MS spectra are included in the resulting feature tables. A minimum of four MS1 data points across a chromatographic peak is

recommended for feature finding with Lipid Annotator. Therefore, the MS/MS acquisition parameters (acquisition rates and number of precursors per cycle) must be optimized to ensure a cycle time that meets this minimum requirement. With the chromatographic method and plasma sample used in this study, we observed the lipid chromatographic base peak widths to range from ~6 to 14 seconds, with an average peak width of ~8 seconds. Therefore, given the minimum observed peak width of six seconds, the MS/MS parameters were adjusted to yield a cycle time of 1.43 seconds. This ensured a minimum of four points across the narrowest chromatographic peaks.

Iterative MS/MS acquisition parameters were found to be important for lipidome annotation coverage, particularly in the case of lipid isomers. In this context, we define lipid isomers as cases where multiple annotated lipid features have

the same sum composition (and same precursor m/z), but different retention times. However, in some of these cases, the MS/MS spectra provided further differentiation of isomers at the constituent level, for instance providing information on the esterified fatty acyl groups (for example, PC 18:2_18:2 versus PC 16:0_20:4). Analysis of plasma resulted in significant numbers of lipid isomers, where 164 out of 355 (positive mode), and 143 of 326 (negative mode) annotated lipids represented lipid isomers. To ensure lipid isomers are not missed in the workflow, the active exclusion window and the iterative RT exclusion tolerance must be set low enough so that closely eluting isomers with the same precursor mass have the opportunity to be triggered for MS/MS. Figure 8 demonstrates a typical scenario for a pair of closely eluting lysophosphatidylcholine (LPC) isomers with narrow peak widths.

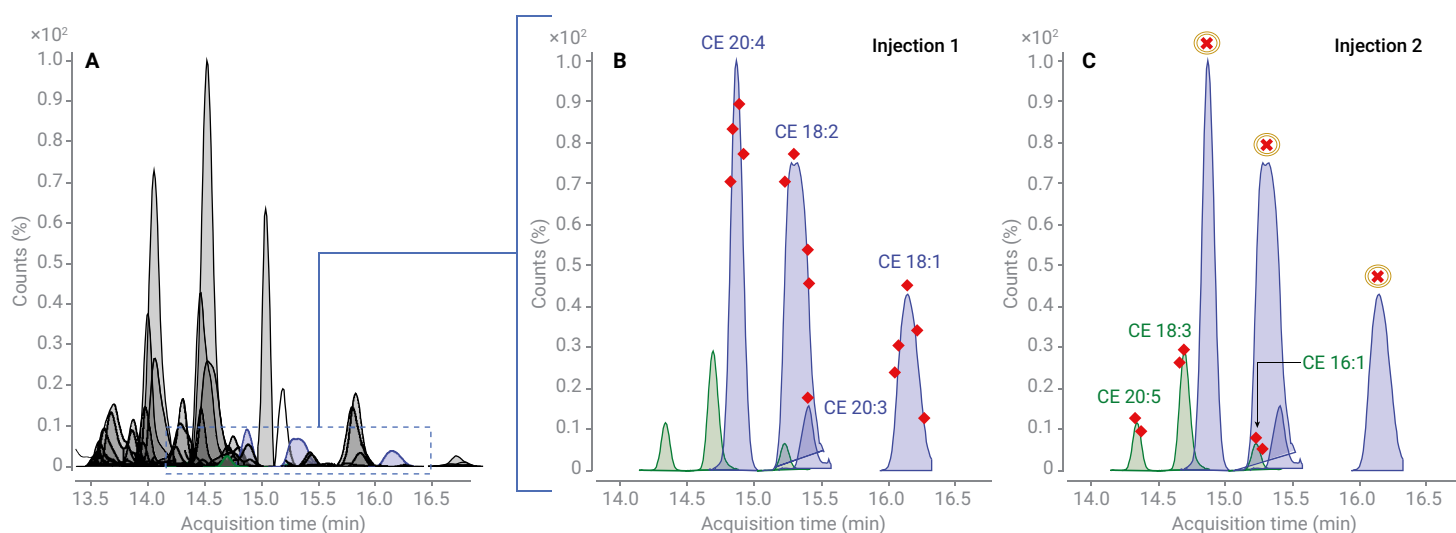


Figure 7. Increased cholesterol ester (CE) precursor selection with Iterative MS/MS from a plasma lipid extract. A) Overlaid extracted MS/MS chromatograms of a retention time region dense with annotated triacylglycerol (TG) lipids (black features). B) Four unique CE lipid precursors (blue features) were selected for fragmentation in the first injection. C) After exclusion of CEs of higher abundance (x symbols) and TGs (not shown), three more unique CE precursors of low abundance (green features) were selected in the subsequent injection. Red diamonds indicate MS1 scans in the chromatograms where the CE $[M+NH_4]^+$ precursors were selected for MS/MS.

Conclusion

This Application Note demonstrates that the Iterative MS/MS mode of LC/Q-TOF data acquisition provides a substantial benefit for improving lipid annotation of complex samples. When applied to a plasma lipid extract, the total number of annotated lipids increased significantly, and lipid classes of low abundance are enriched with Iterative MS/MS.

Lipid Annotator software provides the ability to leverage Iterative MS/MS data to quickly and automatically generate custom PCDL libraries with deep annotation coverage. These libraries with RT information are a critical component of an Agilent lipidomics software workflow that covers targeted and untargeted lipid profiling, from lipid annotation to differential analysis.

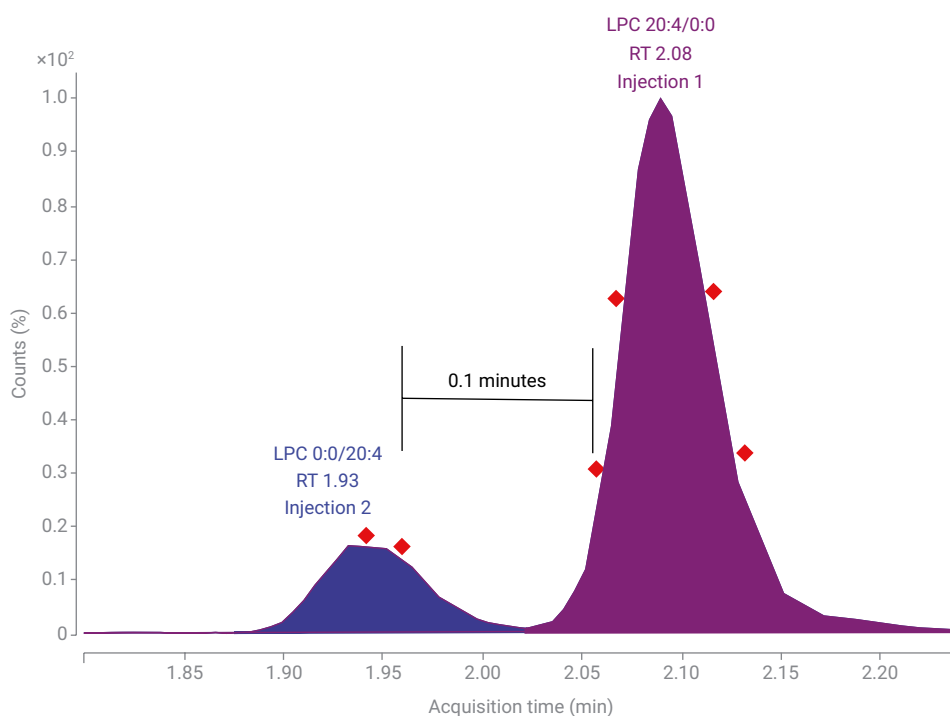


Figure 8. Iterative MS/MS parameters optimized for lipid isomers. Extracted ion chromatograms are shown for two lysophosphatidylcholine (LPC) 20:4 isomers annotated with Lipid Annotator software. The red diamonds indicate hypothetical MS1 scans where the LPC 20:4 $[M+H]^+$ precursor m/z 544.3398 is triggered for MS/MS. Setting the Iterative RT exclusion tolerance to ± 0.1 minutes ensures that the same precursor m/z (± 20 ppm) of the neighboring LPC isomer was picked for MS/MS in subsequent injections.

References

1. Cajka, T.; Fiehn, O. LC/MS Method for Comprehensive Analysis of Plasma Lipids. *Agilent Technologies Application Note*, publication number 5991-9280, **2018**.
2. Sartain, M.; Sana, T. Impact of Chromatography on Lipid Profiling of Liver Tissue Extracts. *Agilent Technologies Application Note*, publication number 5991-5494, **2015**.
3. Kind, T.; *et al.* LipidBlast *in silico* tandem mass spectrometry database for lipid identification. *Nature Methods* **2013**, *10*(8), 755–758
4. Tsugawa, H.; *et al.* MS-DIAL: data-dependent MS/MS deconvolution for comprehensive metabolome analysis. *Nature Methods* **2015**, *12*(6), 523–526.
5. Wu, L.; Wong, D. L. An Integrated Workflow for Peptide Mapping of Monoclonal Antibodies. *Agilent Technologies Application Note*, publication number 5991-8633, **2017**.

www.agilent.com/chem

For Research Use Only. Not for use in diagnostic procedures.

This information is subject to change without notice.

© Agilent Technologies, Inc. 2019
Printed in the USA, March 26, 2019
5994-0775EN

 **Agilent**
Trusted Answers

Application Note

Lipidomics



Lipid Profiling Workflow Demonstrates Disrupted Lipogenesis Induced with Drug Treatment in Leukemia Cells

Using an Agilent 6546 LC/Q-TOF and
MassHunter Lipid Annotator Software

Authors

Mark Sartain,
Genevieve Van de Bittner, and
Sarah Stow
Agilent Technologies, Inc.
Santa Clara, CA

Abstract

The Agilent lipidomics profiling workflow, using the Agilent 6546 LC/Q-TOF and Agilent MassHunter Lipid Annotator software, was applied to the study of drug-treated acute myeloid leukemia (AML) cells. The results confirmed previously reported observations, and revealed lipid differences made evident through the expanded coverage of this comprehensive workflow.

Introduction

A previous study found that a drug combination (BaP) of the lipid-lowering drug bezafibrate (BEZ) and the contraceptive medroxyprogesterone acetate (MPA) had potent anticancer properties for AML, an aggressive blood cancer.¹ The authors further showed with a series of experiments, including lipid analysis, that BaP slows *de novo* fatty acid and phospholipid biosynthesis through downregulation of lipogenic enzymes, and suggested dysregulation of lipogenesis as a major contributor to the anticancer effect of BaP.

As a proof-of-principle study, we applied a lipidomics profiling workflow to analyze lipid alterations in the AML K562 cell line in response to BEZ, MPA, and the BaP drug combination. The Agilent lipid analysis workflow was performed with the 6546 LC/Q-TOF, a mass spectrometer designed to have wide dynamic range while simultaneously providing improved resolution independent of acquisition rate. Key to the workflow is MassHunter Lipid Annotator software, which quickly annotates lipid MS/MS spectra and easily generates a custom library of detected lipids, with deep annotation coverage. These libraries are a critical component of the complete lipid analysis workflow, and support targeted and untargeted lipidomics profiling.

Experimental

Cell culture

AML K562 cells were cultured in supplemented RPMI medium. Six-well plates were seeded with 2.4×10^5 cells/mL (3 mL/well) and four different treatments were applied: 0.5 mM BEZ, 5 mM MPA, BaP (a combination of 0.5 mM BEZ and 5 mM MPA), or vehicle control (1:1 ethanol/DMSO).

Four replicate wells were prepared for each treatment. After incubation for 24 hours, cells were pelleted by centrifugation, washed with PBS (–Ca, –Mg, 1 mL, 4 °C), repelleted, flash-frozen, and stored at –80 °C. Figure 1 depicts the cell culture strategy.

Lipid extraction

Cell pellets were thawed on ice, and lipids were extracted with a modified Folch extraction procedure. Methanol (200 μ L) was added to each cell pellet in a 2 mL Eppendorf tube, and tubes were mixed using a vortex mixer for two minutes. Chloroform (400 μ L) was

added, and tubes were mixed using a vortex mixer for two minutes. To induce phase partitioning, 120 μ L of water was added to each sample. The mixture was then mixed with a vortex mixer for two minutes, and centrifuged at $16,000 \times g$ for five minutes at 4 °C. The lower layer was carefully removed with a gas-tight glass syringe, and transferred to a second Eppendorf tube. To re-extract the remaining interphase and upper phase layers, 450 μ L of a chloroform/methanol/water (86:14:1, v/v/v) mixture was added, mixed with a vortex mixer for two minutes, and centrifuged again.

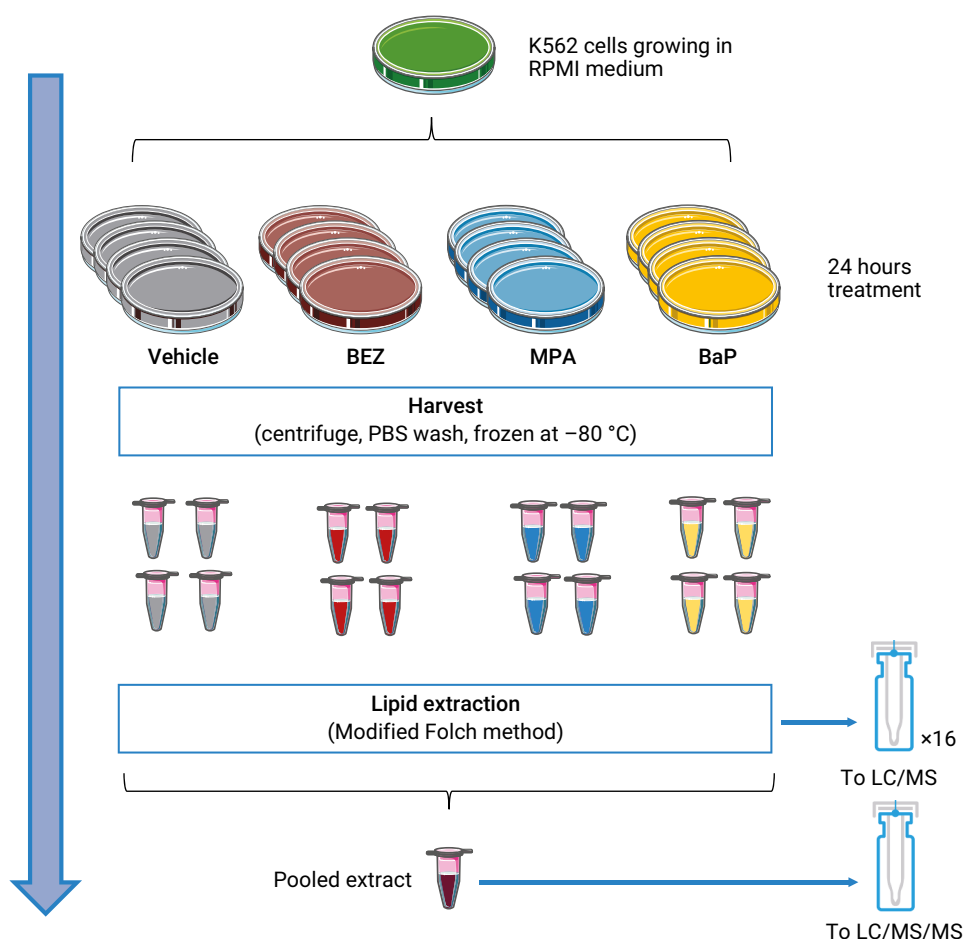


Figure 1. Experimental design for studying effects of drug treatments on cancer cell lipidome.

The lower layers were combined, and 600 µL of a chloroform/methanol/water (3:48:47 v/v/v) mixture was added, the solutions were then mixed using a vortex mixer for two minutes and centrifuged. The lower layer was transferred to a fresh Eppendorf tube, dried by a vacuum concentrator, resuspended with 200 µL of reconstitution solvent (methanol/chloroform (9:1 v/v)), and briefly mixed with a vortex mixer. Extracts were divided and concentrated for different LC/MS acquisition methods as follows:

- Samples for positive ion mode LC/MS:
 1. Fifty microliters of the extracts were transferred to deactivated glass vial inserts for MS1 data acquisition on the individual replicates.
 2. Ten-microliter aliquots from each of the 50 µL samples were combined in a single glass vial insert (16 samples = 160 µL). The pooled aliquot was concentrated by drying in a vacuum concentrator and resuspended in 50 µL of reconstitution solvent for AutoMS/MS (Iterative MS/MS) data acquisition.
- Samples for negative-ion mode LC/MS:
 1. The remaining 150 µL of each extract was transferred to a deactivated glass vial insert and dried by a vacuum concentrator. The samples were resuspended in 50 µL of reconstitution solvent for MS1 data acquisition on the individual replicates.

2. Ten-microliter aliquots from each of the reconstituted 50 µL samples were combined in a single glass vial insert (16 samples = 160 µL). The pooled aliquot was concentrated by drying in a vacuum concentrator and resuspended in 50 µL of reconstitution solvent for AutoMS/MS (Iterative MS/MS) data acquisition.

- Five-microliter injections were made for all samples.

Instrumentation

- **LC system:** Agilent 1290 Infinity II LC including:
 - Agilent 1290 Infinity II High Speed Pump (G7120A)
 - Agilent 1290 Infinity II Vialsampler with thermostat (G7129B)
 - Agilent 1290 Infinity II Multicolumn Thermostat (G7116B)

- **MS system:** Agilent 6546 LC/Q-TOF with an Agilent Jet Stream technology ion source

Method

A pooled K562 lipid extract representing the 16 samples (four conditions × four replicates) was acquired by Iterative MS/MS, a fully automated Q-TOF acquisition mode in which a sample is injected multiple times, and precursors selected for MS/MS fragmentation in the previous injections are excluded on a rolling basis. The value of Iterative MS/MS in obtaining larger numbers of lipid annotations from a single sample was demonstrated previously.²

Detailed experimental methods for chromatography and AutoMS/MS mass spectrometry were followed as described;² parameters are provided in Tables 1 and 2. Additionally, MS-only data were acquired on the individual samples, with an MS acquisition rate of three spectra/second.

Table 1. Chromatographic conditions.

Parameter	Agilent 1290 Infinity II LC																		
Analytical Column	Agilent InfinityLab Poroshell 120 EC-C18, 3.0 × 100 mm, 2.7 µm (p/n 695975-302)																		
Guard Column	Agilent InfinityLab Poroshell 120 EC-C18, 3.0 × 5 mm, 2.7 µm (p/n 823750-911)																		
Column Temperature	50 °C																		
Injection Volume	5 µL																		
Autosampler Temperature	4 °C																		
Needle Wash	15 seconds in wash port (50:50 methanol/isopropanol)																		
Mobile Phase	A) 10 mM ammonium acetate, 0.2 mM ammonium fluoride in 9:1 water/methanol B) 10 mM ammonium acetate, 0.2 mM ammonium fluoride in 2:3:5 acetonitrile/methanol/isopropanol																		
Flow Rate	0.6 mL/min																		
Gradient Program	<table border="1"> <thead> <tr> <th>Time</th> <th>%B</th> </tr> </thead> <tbody> <tr><td>0.00</td><td>70</td></tr> <tr><td>1.00</td><td>70</td></tr> <tr><td>3.50</td><td>86</td></tr> <tr><td>10.00</td><td>86</td></tr> <tr><td>11.00</td><td>100</td></tr> <tr><td>17.00</td><td>100</td></tr> <tr><td>17.10</td><td>70</td></tr> <tr><td>19.00</td><td>70</td></tr> </tbody> </table>	Time	%B	0.00	70	1.00	70	3.50	86	10.00	86	11.00	100	17.00	100	17.10	70	19.00	70
Time	%B																		
0.00	70																		
1.00	70																		
3.50	86																		
10.00	86																		
11.00	100																		
17.00	100																		
17.10	70																		
19.00	70																		
Stop Time	19 minutes																		
Post Time	None																		
Observed Column Pressure	170 to 330 bar																		

Software

- Agilent MassHunter Q-TOF Data Acquisition Version 10.0 was used to operate the 6546 LC/Q-TOF.
- Agilent MassHunter Lipid Annotator Version 1.0 with default method parameters was used, except only $[M+H]^+$ and $[M+NH_4]^+$ precursors were considered for positive ion mode analysis, and only $[M-H]^-$ and $[M+HAc-H]^-$ precursors were considered for negative ion mode analysis.
- Agilent MassHunter PCDL Manager Version B.08 SP1 was used to manage and edit the exported annotated lipid libraries (PCDL). Specifically, PCDL Manager was used to remove redundancies for nine Cer_NS lipids, where separate entries were observed for $[M-H]^-$ and $[M+acetate]^-$ molecular ions. The $[M-H]^-$ Cer_NS entries were deleted, leaving 653 lipids in the negative ion mode PCDL.
- Agilent MassHunter Profinder Version 10.0 was used for feature extraction.³ The provided "Profinder - Lipids.m" method was used for batch targeted feature extraction with the following changes:

- Step 1:** +H and +NH₄ checked (pos), -H and +CH₃COO checked (neg); report single ions or single-ion features with charge state z = 1: checked
- Step 2:** Expected data variation for MS isotope abundance: 12.5%
- Step 3:** Smoothing function: Quadratic/Cubic Savitzky-Golay with function width 8; height filter: uncheck; limit to largest (by height) to maximum: 10 peaks

Table 2. Agilent 6546 LC/Q-TOF AutoMS/MS (Iterative) parameters.

Parameter	Agilent 6546 LC/Q-TOF
Gas Temperature	200 °C
Gas Flow	10 L/min
Nebulizer (psig)	50
Sheath Gas Temperature	300 °C
Sheath Gas Flow	12 L/min
VCap	3,500 V (+), 3,000 V (-)
Nozzle Voltage	0 V
Fragmentor	150 V
Skimmer	65 V
OctopoleRF Vpp	750 V
Reference Mass	<i>m/z</i> 121.050873, <i>m/z</i> 1221.990637 (+) <i>m/z</i> 119.03632, <i>m/z</i> 980.016375 (-)
MS and MS/MS Range	<i>m/z</i> 40 to 1,700 (+)
Minimum MS and MS/MS Acquisition Rate	3 spectra/s
Isolation Width	Narrow (~1.3 <i>m/z</i>)
Collision Energy	20 eV (+), 25 eV (-)
Maximum Precursors Per Cycle	3
Precursor Abundance-Based Scan Speed	Yes, target 25,000 counts/spectrum
Use MS/MS Accumulation Time Limit	Yes
Reject Precursors that Cannot Reach Target TIC	No
Threshold for MS/MS	5,000 counts and 0.001 %
Active Exclusion Enabled	Yes, one repeat, then exclude for 0.05 minutes
Purity	Stringency 70%, cutoff 0%
Isotope Model	Common organic molecules
Sort Precursors	1, 2, unknown
Static Exclusion Ranges	<i>m/z</i> 40 to 151 (+) <i>m/z</i> 40 to 210 (-)
Iterative MS/MS Mass Error Tolerance	20 ppm
Iterative MS/MS RT Exclusion Tolerance	±0.1 minutes

- Step 4:** Unchanged Step 5 uncheck Score (Tgt)
- Agilent MassHunter Mass Profiler Professional Version 15.1 was used for differential analysis. Two experiments (positive or negative ion) were created with the "Lipidomics" experiment type, and the corresponding Profinder archives (.pfa) were used as the data source. A percentile shift normalization algorithm (75 %) was used, and datasets were baselined to the median of all samples.
- Agilent MassHunter ID Browser Version 10.0 was used within MPP to make annotations in the untargeted workflow, with masses ±5 ppm and retention times ±0.10 minutes as required criteria.

Workflow

Both the targeted and untargeted lipidomics workflows were used as previously described.⁴

Results and discussion

Lipid Annotator database creation with pooled AML cellular lipid extracts

As the first step in the lipidomics workflow, two sets of five iterative MS/MS data files from pooled AML cell extracts were analyzed with Lipid Annotator software (Figure 2). There were 430 lipids representing 17 classes annotated for positive ion mode, and 653 lipids representing 25 classes annotated for negative ion mode. Lipid Annotator results were exported to PCDL (.cdb) files.

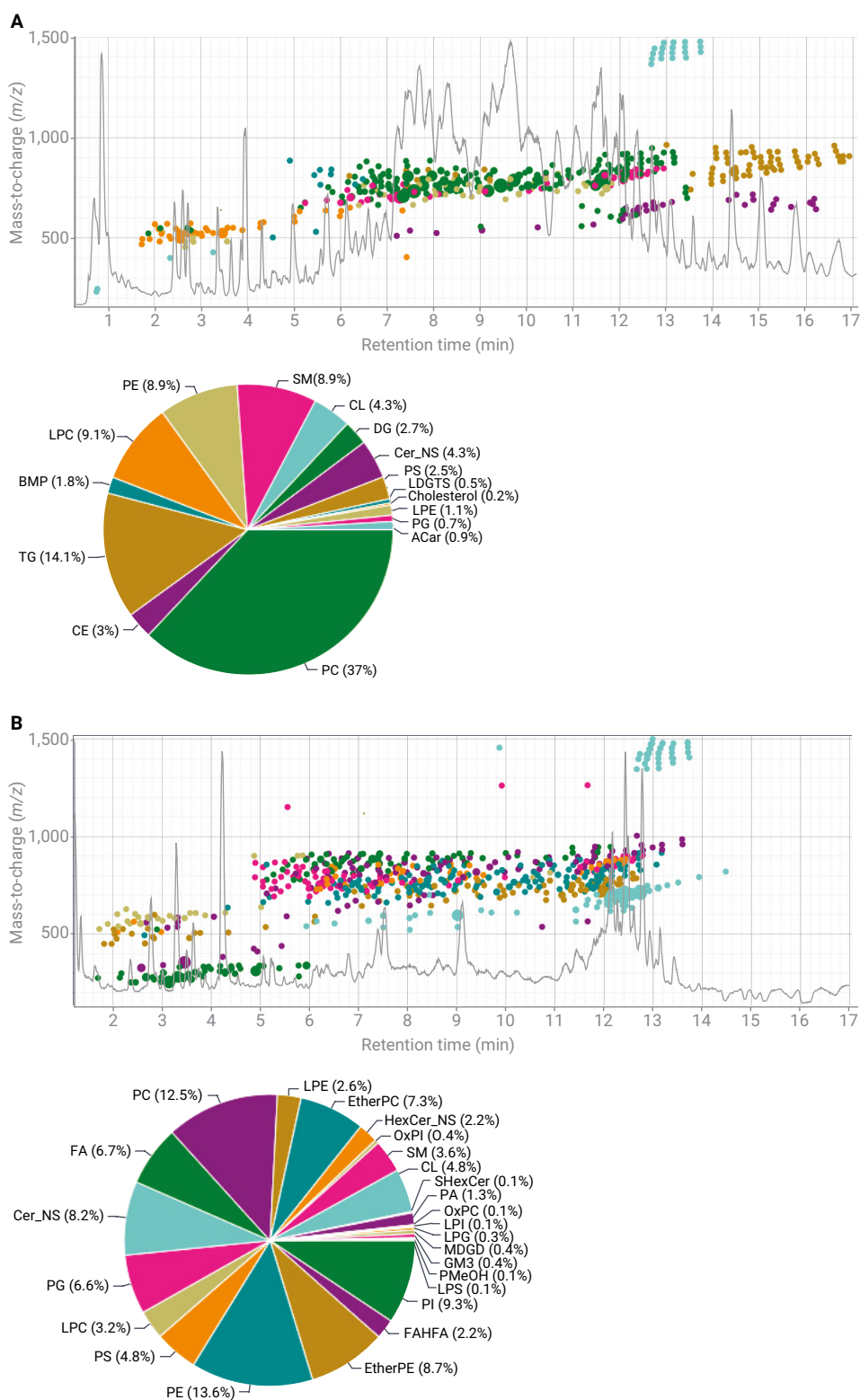


Figure 2. Lipid Annotator software results for positive (A) and negative (B) ionization modes. Five iterative MS/MS data files were analyzed as a batch for each project. For illustration purposes, a representative total ion chromatogram is overlaid with the m/z versus retention time scatter plot. Lipid features are colored by lipid class corresponding to the pie charts, where the numbers of annotated lipids are shown as percentages.

Lipid profiling identifies perturbations induced with drug treatments

The PCDL (.cdb) databases were used for Batch Targeted Feature Extraction in Profinder on the respective batches of 16 MS1 data files. Critically, both the database compound formulas and retention times were used as required criteria to search the MS1 data files for the lipid features in a targeted manner. Resulting compounds were reviewed in Profinder and, in some cases, features were manually integrated or removed due to poor or ambiguous feature peak shapes. After manual curation, 375 compounds and 548 compounds remained in the positive and negative ion mode datasets, respectively. Profinder results (.pfa file) were imported into Mass Profiler Professional (MPP) for statistical analysis, where separate experiments were created for positive and negative ion modes. After normalization and baselining, the resulting PCA plots for both polarities were similar. Without filtering of entities (keeping all compounds), the results showed tight clustering of the biological replicates within each condition and demonstrated clear differences between the drug treatments. Both BEZ and MPA contributed separately to the combination BaP effect (Figure 3). Separation of the groups along principal component 1 suggested that BEZ treatment contributed more than MPA to the combination BaP drug effect on the lipidome. These observations were consistent with those described previously.¹

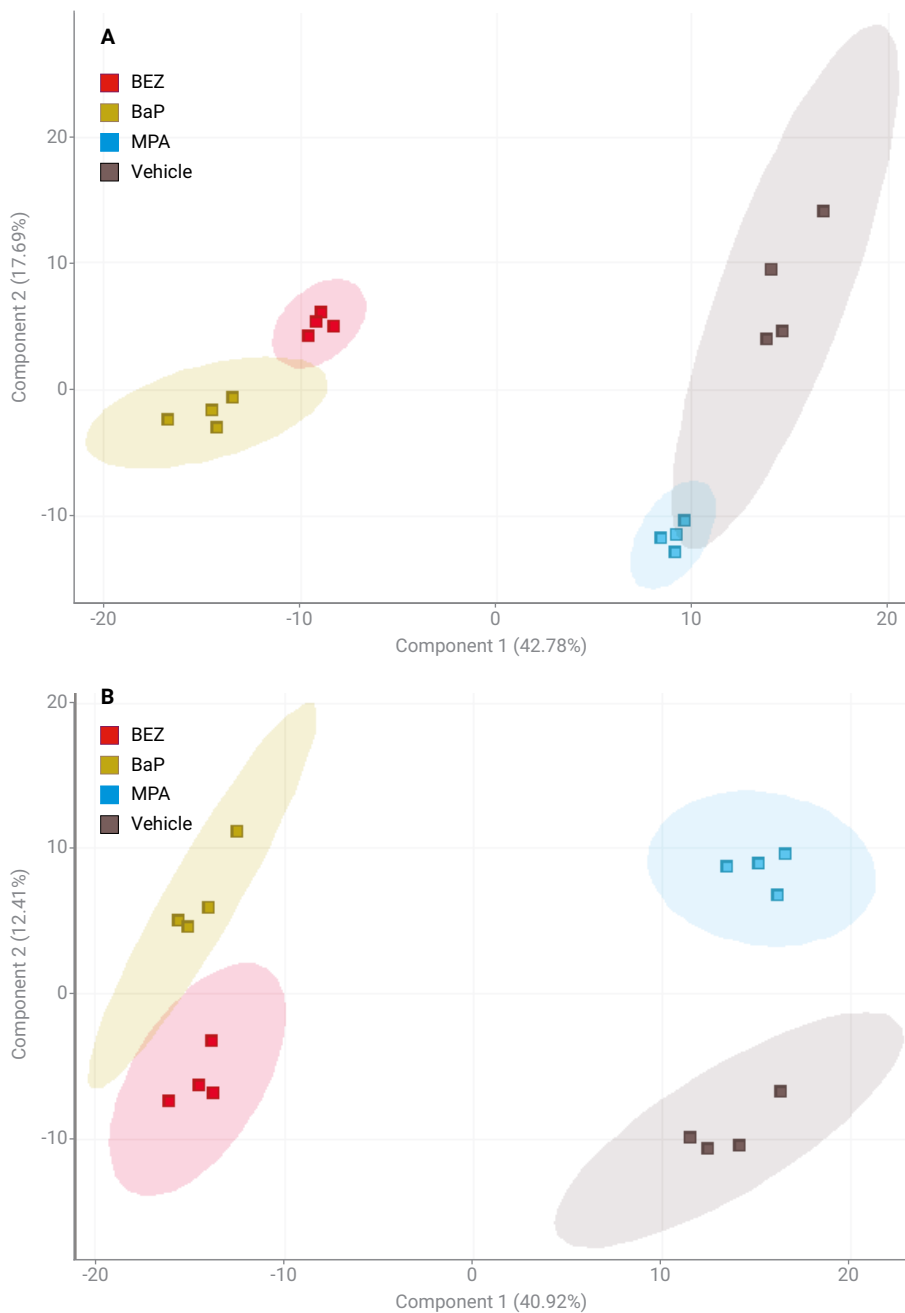


Figure 3. PCA plots for the positive ion (A) and negative ion (B) datasets.

Sample correlation (not shown) and unsupervised hierarchical clustering (Figure 4) provided further support for the PCA results. Biological replicates within the conditions grouped together, and BEZ samples showed a closer relationship to BaP than MPA samples. Trends were also observed from unsupervised clustering on the annotated lipid features. For example, inspection of the cluster tree within a region showing a clear pattern revealed a close relationship for many triacylglycerol (TG) lipids. These lipids were increased in BEZ and BaP treatments compared to MPA and the vehicle control samples.

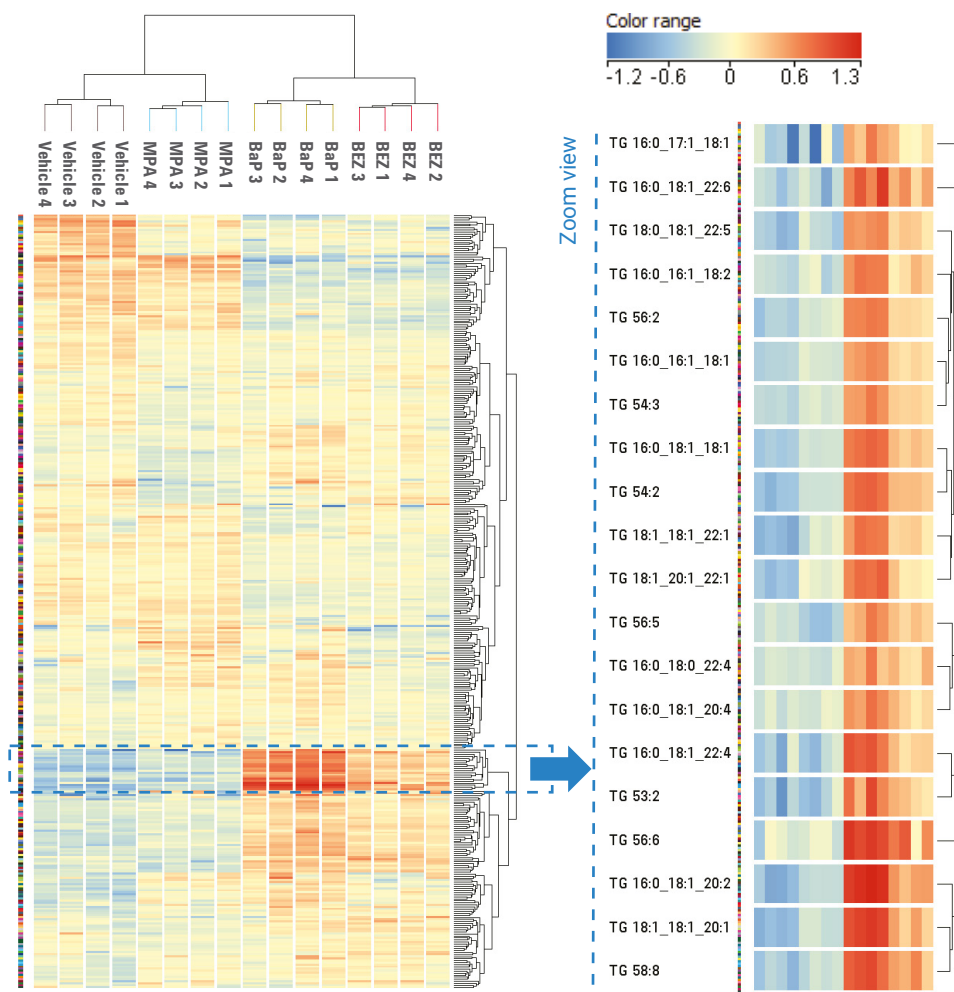


Figure 4. Combined unsupervised hierarchical clustering results on compounds ($n = 375$) and conditions for the positive ion dataset. (Right) A zoomed region of the cluster tree enriched with annotated TG lipids is shown. The color range represents the normalized, transformed abundances for each TG feature represented on a \log_2 scale.

Lipid profiling demonstrates disrupted lipogenesis

To assess differences across lipid class abundances in more detail, a lipid class matrix plot (heat map) was created in MPP from the positive ion mode dataset (Figure 5). Clear differences were observed. In agreement with Southam *et al.*,¹ TGs were increased and diacylglycerols (DGs) were decreased in BaP versus vehicle control. DGs are intermediates in the *de novo* phospholipid biosynthetic pathway, and the authors suggested that DG depletion with BaP treatment resulted from disruption of phospholipid synthesis at the acyl chain addition stage. Table 3 shows a summary of lipid classes with significantly different abundances from the positive and negative ion datasets.

In contrast to the previous report, we did not observe a significant decrease of lysophosphatidylcholine (LPC) or lysophosphatidylethanolamine (LPE) class abundances with BaP treatment. Multiple reasons could account for this discrepancy, including differences in normalization and processing methods for the MS lipid datasets. We observed significant lipid class differences not reported in the previous study, most notably increases in levels of ceramide nonhydroxyfatty acid-sphingosines (Cer_NS) and hexosylceramide nonhydroxyfatty acid-sphingosines (HexCer_NS), and decreased phosphatidylcholine (PC) levels in BaP treated cells versus vehicle control. While the previous study applied a shotgun lipidomics approach with targeted scans for a limited panel of lipid classes, our targeted workflow began with a discovery phase to search a comprehensive *in silico* spectral library, and then used these results for targeted data mining. Therefore, our approach was unrestricted, and likely led to these findings in lipid class differences.

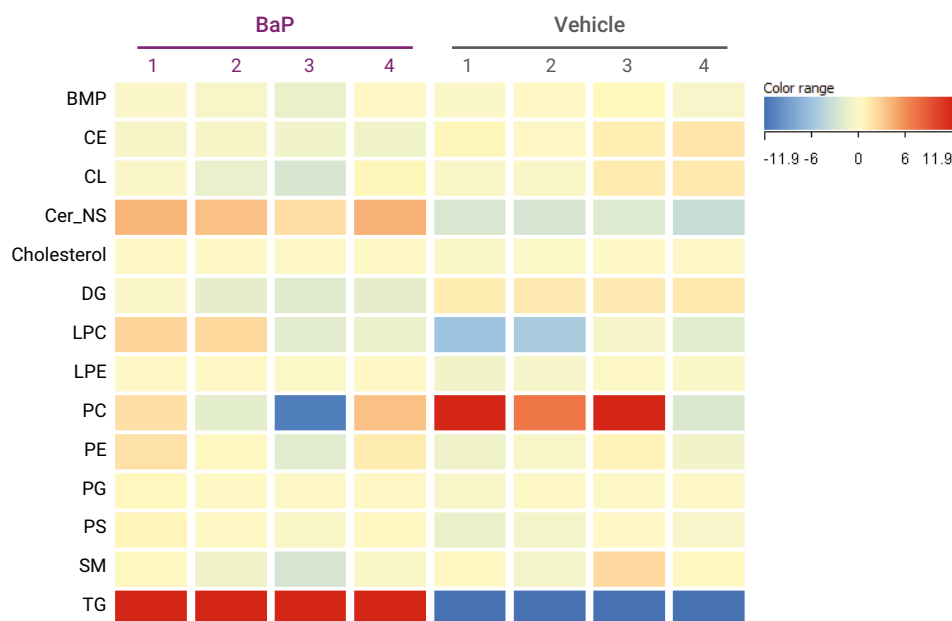


Figure 5. MPP lipid class matrix of total normalized lipid class abundances across BaP treatment and vehicle control sample replicates. The color range represents the sum of normalized, transformed abundances for all lipid features within a lipid class.

Table 3. Summary of lipid classes with significantly different abundance levels induced with BaP treatment.

Lipid Class	Abbreviation	BaP Effect	Polarity [†]
Ceramide Nonhydroxyfatty Acid-Sphingosines	Cer_NS	Increased	(+)***, (-)*
Hexosylceramide Nonhydroxyfatty Acid-Sphingosines	HexCer_NS	Increased	(-)***
Triacylglycerols	TG	Increased	(+)***
Gangliosides	GM3	Increased	(-)**
Lyso-Phosphatidylglycerols	LPG	Increased	(-)**
Ether-Linked Phosphatidylcholines	Ether PC	Increased	(-)*
Lyso-Phosphatidylethanolamines	LPE	Increased	(+)*
Lyso-Phosphatidylserines	LPS	Increased	(-)*
Sulfatides	SHexCer	Increased	(-)*
Diacylglycerols	DG	Decreased	(+)***
Monogalactosyldiacylglycerols	MGDG	Decreased	(-)***
Phosphatidylinositols	PI	Decreased	(-)***
Cholesterol Esters	CE	Decreased	(+)**
Cardiolipins	CL	Decreased	(-)**
Oxidized Phosphatidylcholines	OxPC	Decreased	(-)*
Oxidized Phosphatidylinositols	OxPI	Decreased	(-)*
Phosphatidic Acids	PA	Decreased	(-)*

[†] A two-tailed t-test was used to determine significance between vehicle and BaP sample groups:

* p < 0.05, ** p < 0.01, *** p < 0.001

Lipid matrices were also created in MPP to visualize abundance differences across individual lipid features within lipid classes. Inspection of the phosphatidylcholine (PC) matrix plot revealed some inverse patterns corresponding to a decrease in PCs with saturated fatty acyl chains (for example, PC 16:0_26:0) and an increase in PCs with polyunsaturated fatty acyl chains (for example, PC 18:1_22:6) induced with BaP treatment (Figure 6). These observations are also consistent with Southam *et al.*,¹ who suggested that PC lipids with 0 to 2 double bonds are decreased due to reduced *de novo* fatty acid and phospholipid synthesis induced by BaP treatment. They further hypothesized that the increase in polyunsaturated PC lipids was most likely due to cells obtaining polyunsaturated fatty acids from an exogenous source other than glucose.

Differential response of lipid isomers with drug treatment

The comprehensive LC-based lipidomics approach allowed profiling of lipid isomers that had the same sum composition (that is, same exact mass) but were resolved with chromatography. There were significant numbers of such isomers in the datasets: in the positive mode dataset, 94 of the 430 annotated lipids were isomers, while in the negative mode dataset, 165 of 653 annotated lipids were isomers. In many cases, isomers showed markedly different responses to drug treatment. Inspection of the ceramide (Cer_NS) lipid matrix in MPP revealed an inverse relationship for several pairs of isomers (Figure 7A). As an example, extracted ion chromatograms for the pair of partially resolved Cer_NS 42:2 isomers confirmed an inverse response to BaP treatment, where the later-eluting isomer was decreased in BaP treatment compared to the early-eluting isomer (Figure 7B).

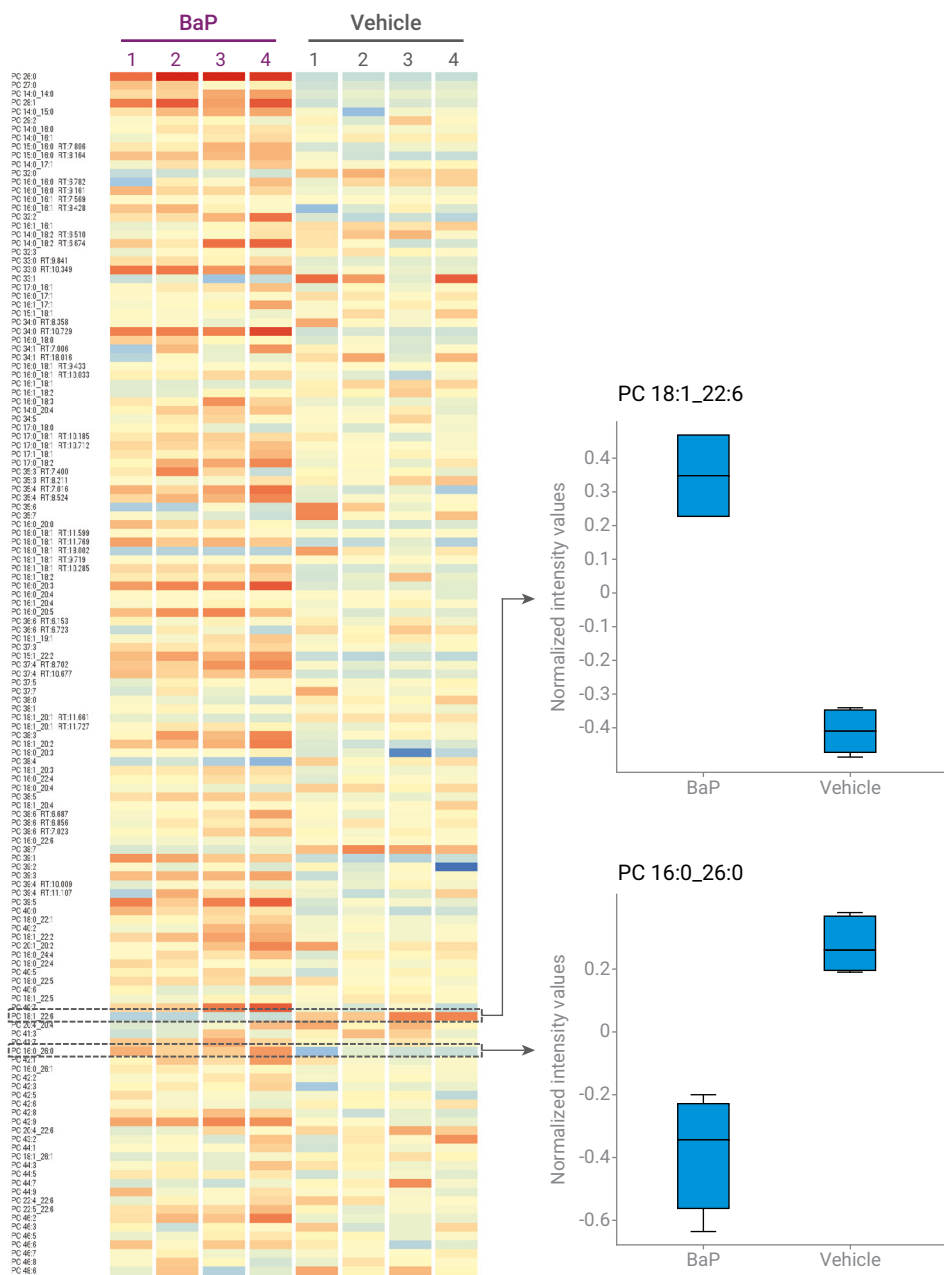


Figure 6. MPP lipid matrix of 137 phosphatidylcholine (PC) lipid features across BaP treatment and vehicle control sample replicates. Box and whisker plots of two selected PC features are shown to the right.

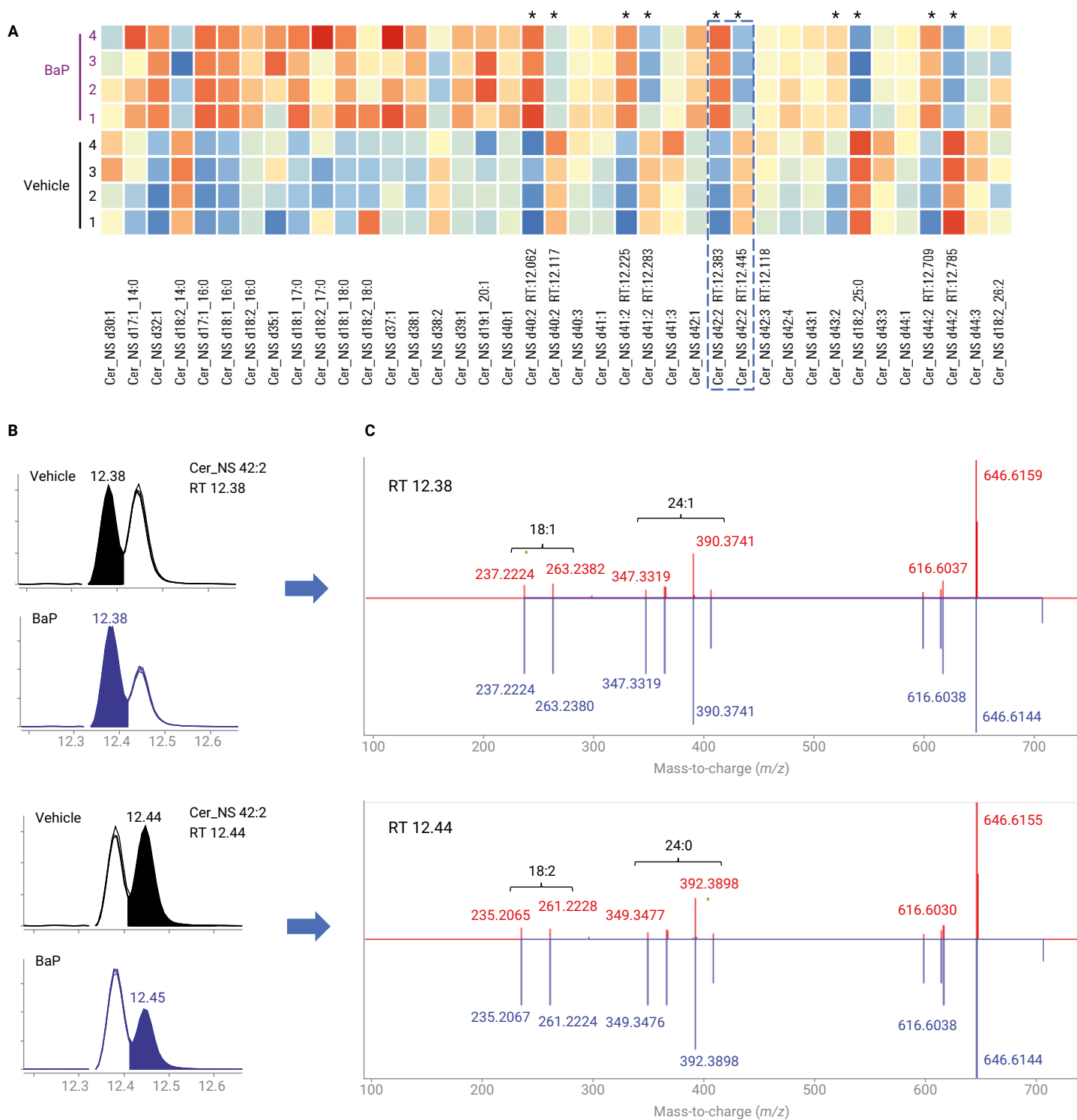


Figure 7. Differential responses and structural elucidation of ceramide nonhydroxyfatty acid-sphingosine (Cer_NS) isomers. (A) MPP lipid matrix of 39 Cer_NS lipid features across BaP treatment and vehicle control sample replicates. Pairs of isomers indicated with asterisks have the same exact mass but different retention times and showed an inverse response. (B) Overlaid extracted ion chromatograms comparing vehicle control (n = 4) to BaP treatment (n = 4) for the pair of Cer_NS 42:2 isomers. (C) Corresponding head-to-tail plots from Lipid Annotator with the major matched product ions additionally labeled (observed, red; database values, blue). Product ion shifts of plus or minus m/z 2.0156 between the two plots provided the evidence for the difference in the double bond numbers in the sphingosine bases and esterified fatty acids (labeled). The observed spectra matched Cer_NS d18:1_24:1 and Cer_NS d18:2_24:0 database spectra, and these were indicated as the most likely constituents in the Lipid Annotator software.

While the isomers were annotated with the same sum composition, inspection of Lipid Annotator results provided strong evidence that the early- and late-eluting isomers were Cer_NS d18:1_24:1 and Cer_NS d18:2_24:0, respectively (Figure 7C). The biological significance of the differential response of ceramide isomers to BaP treatment is not known, but this type of information is only revealed with the lipidomics profiling approach.

The untargeted lipidomics workflow reveals a highly differential atypical lipid

As described elsewhere,⁴ untargeted workflows are also supported and use the same PCDL and software as the targeted workflow previously described. The major differences are that:

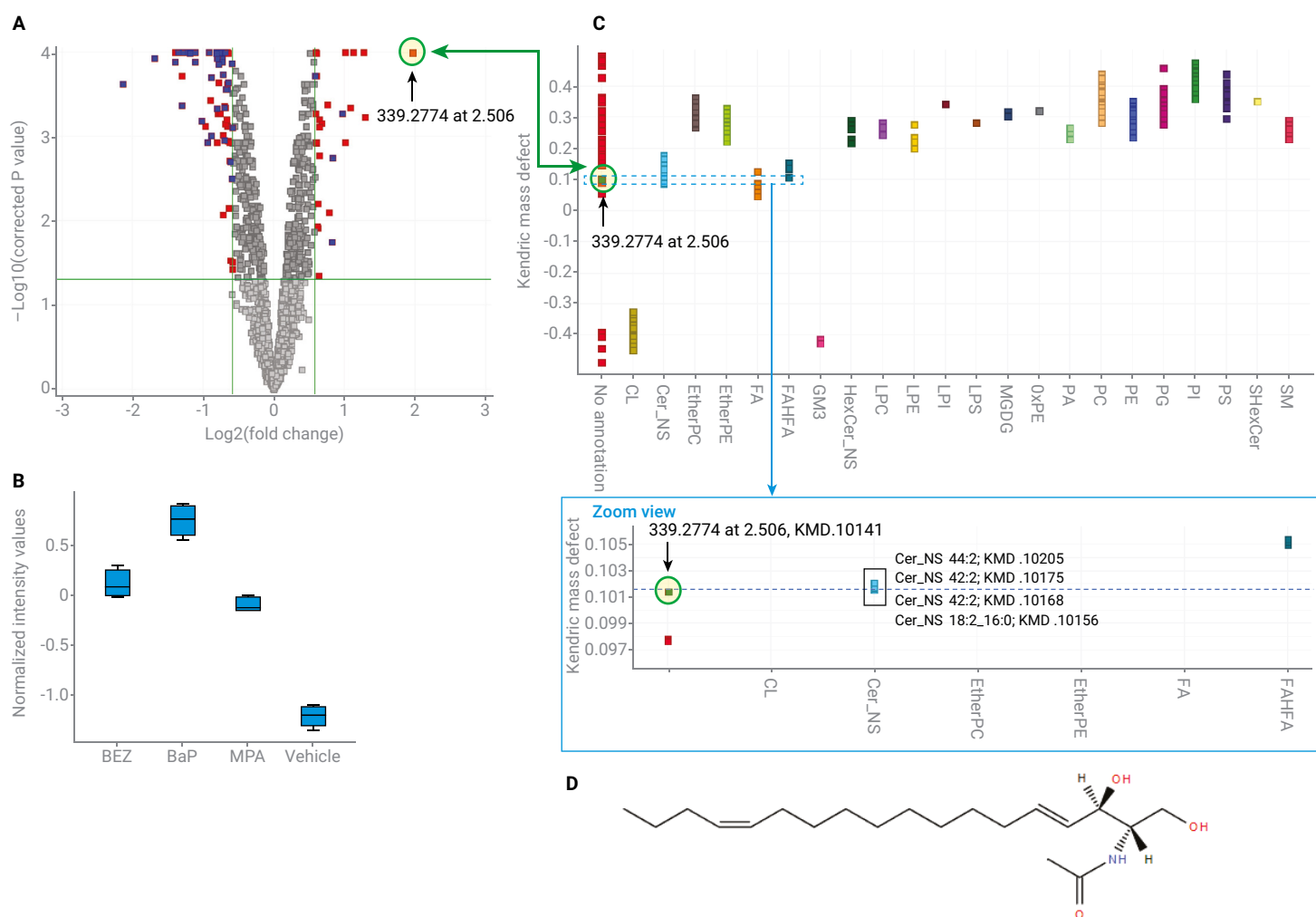
- Untargeted feature finding (recursive batch feature extraction algorithm) in Profinder is used, and
- Lipid annotation is performed later in the workflow within MPP using the ID Browser tool.

In our study, the 16 negative ion MS1 data files were analyzed with the recursive batch feature extraction algorithm in Profinder, and 2,052 features were imported into MPP. As a result, 513 out of the 2,052 features were annotated as lipids with the ID Browser tool using the same negative-ion PCDL library created above (RT \pm 0.10 minutes was specified as the required criteria).

To focus the differential analysis on reproducible features, the entity list was filtered by sample variability with a CV <25% required for all four conditions. This reduced the entity list to 1,377 features. A moderated t-test on BaP treatment versus vehicle control resulted in 93 entities that were significantly different (fold-change cutoff 1.5, p-value 0.05), and 41 of these entities had been annotated as lipids (Figure 8A). The most highly differential feature showed a 3.93-fold increase in BaP cells compared to vehicle control (p-value 3.54×10^{-5}), and inspection of the entity showed striking differences across the four conditions (Figure 8B). The compound of interest had a neutral mass of 339.2774 Da, and ID Browser did not return an annotation.

To gain insight into the nature of this compound, a Kendrick mass defect (KMD) plot was created in MPP for the combined list of 513 annotated lipids and the 93 differential entities (Figure 8C). Plotting KMD (Y-axis) against lipid class (X-axis) revealed that the feature of interest shared a similar KMD to a group of four Cer_NS lipids each with two double bonds. Interestingly, the masses of the four ceramide lipids (masses 707 to 735 Da) were much larger than the feature of interest (339 Da). The Lipid Calculator tool within Lipid Annotator was used to generate hypothetical Cer_NS lipids to assess whether a sum composition could be generated with a resulting mass close

to m/z 339.2774. With this approach, the lipid Cer_NS d18:2_2:0 showed a mass within 0.3 ppm of the observed feature mass. Furthermore, analysis with Qualitative analysis software showed an MS/MS product ion specific for the d18:2 sphingosine backbone that provided further evidence for the candidate Cer_NS d18:2_2:0 annotation (data not shown). The candidate structure for Cer_NS d18:2_2:0, also known as C2 ceramide or N-acetylsphingosine, is shown in Figure 8D. This C2 ceramide is absent in many lipid databases (including Lipid Annotator) and, to our understanding, has not routinely been identified in lipidomics studies. However, C2 ceramide was found physiologically at low levels in a different AML cell line (HL-60).⁵ Synthetic C2 ceramide is widely used as a research tool for its biologically active properties, including the ability to inhibit cell proliferation and induce apoptosis.⁶ We speculate the increase of C2 ceramide in the BaP-treated cells could be related to the anticancer effects of BaP, and believe this information may be of interest to the cancer research community.



Conclusion

This Application Note demonstrates that the lipidomics profiling workflow, including Lipid Annotator software, provides substantial improvement in lipid annotation and differential analysis of complex samples. We applied a targeted workflow to study lipidome alterations of the acute myeloid leukemia K562 cell line in response to a combination of the BEZ and MPA drug candidates. The resulting analysis revealed several cellular changes in response to drug treatment, including a decrease in diacylglycerols, an increase in triacylglycerols, and differences in fatty acyl components. Taken together, these results support a previous report suggesting that the BaP combination may exert its anticancer properties through disruption of lipogenesis.

This lipid profiling workflow also provides more comprehensive lipid annotation than can be achieved by traditional shotgun-based lipidomics approaches. Specifically, we identified significant differences in lipid class abundances induced with BaP treatment that were not previously reported. We also identified specific cases of chromatographically separated lipid isomers that displayed differential responses to drug treatment. Finally, with an untargeted approach we demonstrated the ability to propose candidate annotations for unannotated lipid features using supplementary tools.

References

1. Southam, A. D. *et al.* Drug Redeployment to Kill Leukemia and Lymphoma Cells by Disrupting SCD1-Mediated Synthesis of Monounsaturated Fatty Acids. *Cancer Res.* **2015**, *75*(12), 2530–2540.
2. Sartain, M. *et al.* Improving Coverage of the Plasma Lipidome Using Iterative MS/MS Data Acquisition Combined with Lipid Annotator and 6546 LC/Q-TOF. *Agilent Technologies Application Note*, publication number 5991-0775EN, **2019**.
3. MassHunter Profinder: Batch Processing for High-Quality Feature Extraction of Mass Spectrometry Data. *Agilent Technologies Technical Overview*, publication number 5991-3947EN, **2014**.
4. Lipidomics Analysis with Lipid Annotator and Mass Profiler Professional. *Agilent Technologies Technical Overview*, publication number 5994-1111EN, **2019**.
5. Snyder, F. *et al.* Biosynthesis of N-Acetylsphingosine by Platelet-activating Factor: Sphingosine CoA-independent Transacetylase in HL-60 Cells. *The Journal of Biological Chemistry* **1996**, *271*(1), 209–217.
6. Hannun, Y. A. *et al.* Programmed Cell Death Induced by Ceramide. *Science* **1993**, *259*(5102), 1769–1771.

www.agilent.com/chem

For Research Use Only. Not for use in diagnostic procedures.

This information is subject to change without notice.

© Agilent Technologies, Inc. 2019
Printed in the USA, October 25, 2019
5994-1356EN

 **Agilent**
Trusted Answers

Join Dr. Nicola Zamboni, Institute for Molecular System Biology, ETH Zurich, as he discusses trends and challenges in high-throughput metabolomics and ^{13}C metabolic flux analysis in this award-winning on-demand webinar.

For Research Use Only. Not for use in diagnostic procedures.

The journey from metabolomics to me

Nicola Zamboni

Institute of Molecular Systems Biology
Swiss Federal Institute of Technology (ETH) Zurich

Click here
to watch
this webinar



